

Accelerated Article Preview

Antibody Resistance of SARS-CoV-2 Variants B.1.351 and B.1.1.7

Received: 25 January 2021

Accepted: 25 February 2021

Accelerated Article Preview Published
online 8 March 2021

Cite this article as: Wang, P. et al. Antibody Resistance of SARS-CoV-2 Variants B.1.351 and B.1.1.7. *Nature* <https://doi.org/10.1038/s41586-021-03398-2> (2021).

Pengfei Wang, Manoj S. Nair, Lihong Liu, Sho Iketani, Yang Luo, Yicheng Guo, Maple Wang, Jian Yu, Baoshan Zhang, Peter D. Kwong, Barney S. Graham, John R. Mascola, Jennifer Y. Chang, Michael T. Yin, Magdalena Sobieszczyk, Christos A. Kyratsous, Lawrence Shapiro, Zizhang Sheng, Yaoxing Huang & David D. Ho

This is a PDF file of a peer-reviewed paper that has been accepted for publication. Although unedited, the content has been subjected to preliminary formatting. Nature is providing this early version of the typeset paper as a service to our authors and readers. The text and figures will undergo copyediting and a proof review before the paper is published in its final form. Please note that during the production process errors may be discovered which could affect the content, and all legal disclaimers apply.

Antibody Resistance of SARS-CoV-2 Variants B.1.351 and B.1.1.7

<https://doi.org/10.1038/s41586-021-03398-2>

Received: 25 January 2021

Accepted: 25 February 2021

Published online: 8 March 2021

Pengfei Wang^{1,8}, Manoj S. Nair^{1,8}, Lihong Liu^{1,8}, Sho Iketani^{1,2,8}, Yang Luo¹, Yicheng Guo¹, Maple Wang¹, Jian Yu¹, Baoshan Zhang³, Peter D. Kwong^{3,4}, Barney S. Graham³, John R. Mascola³, Jennifer Y. Chang^{1,5}, Michael T. Yin^{1,5}, Magdalena Sobieszczyk^{1,5}, Christos A. Kyratsous⁶, Lawrence Shapiro^{1,4,7}, Zizhang Sheng¹, Yaoxing Huang¹✉ & David D. Ho^{1,2,5}✉

The COVID-19 pandemic has ravaged the globe, and its causative agent, SARS-CoV-2, continues to rage. The prospects of ending this pandemic rest on the development of effective interventions. Single and combination monoclonal antibody (mAb) therapeutics have received emergency use authorization^{1–3}, with more in the pipeline^{4–7}. Furthermore, multiple vaccine constructs have shown promise⁸, including two with ~95% protective efficacy against COVID-19^{9,10}. However, these interventions were directed toward the initial SARS-CoV-2 that emerged in 2019. The recent emergence of new SARS-CoV-2 variants B.1.1.7 in the UK¹¹ and B.1.351 in South Africa¹² is of concern because of their purported ease of transmission and extensive mutations in the spike protein. We now report that B.1.1.7 is refractory to neutralization by most mAbs to the N-terminal domain (NTD) of the spike and relatively resistant to a few mAbs to the receptor-binding domain (RBD). It is not more resistant to convalescent plasma or vaccinee sera. Findings on B.1.351 are more worrisome in that this variant is not only refractory to neutralization by most NTD mAbs but also by multiple individual mAbs to the receptor-binding motif on RBD, largely owing to an E484K mutation. Moreover, B.1.351 is markedly more resistant to neutralization by convalescent plasma (9.4 fold) and vaccinee sera (10.3–12.4 fold). B.1.351 and emergent variants^{13,14} with similar spike mutations present new challenges for mAb therapy and threaten the protective efficacy of current vaccines.

Considerable SARS-CoV-2 evolution has occurred since its initial emergence, including variants with a D614G mutation¹⁵ that have become dominant. Viruses with this mutation alone do not appear to be antigenically distinct, however¹⁶. SARS-CoV-2 B.1.1.7, also known as 501Y.V1 in the GR clade (Extended Data Fig. 1a), emerged in September 2020 in South East England and rapidly became the dominant variant in the UK, possibly due to its enhanced transmissibility¹¹. This strain has now spread to over 50 countries, and there are indications that it may be more virulent¹⁷. B.1.1.7 contains 8 spike mutations in addition to D614G, including two deletions (69–70del & 144del) in NTD, one mutation (N501Y) in RBD, and one mutation (P681H) near the furin cleavage site (Extended Data Fig. 1b). SARS-CoV-2 B.1.351, also known as 501Y.V2 in the GH clade (Extended Data Fig. 1a), emerged in late 2020 in Eastern Cape, South Africa (SA)¹². This variant has since become dominant locally, raising the specter that it too has enhanced transmissibility. B.1.351 contains 9 spike mutations in addition to D614G, including a cluster of mutations (e.g., 242–244del & R246I) in NTD, three mutations (K417N, E484K, & N501Y) in RBD, and one mutation (A701V) near the furin cleavage site (Extended Data Fig. 1b). There is a growing

concern that these new variants could impair the efficacy of current mAb therapies or vaccines, because many of the mutations reside in the antigenic supersite in NTD^{18,19} or in the ACE2-binding site (also known as the receptor-binding motif–RBM) that is a major target of potent virus-neutralizing antibodies. We therefore addressed this concern by assessing the susceptibility of authentic B.1.1.7 and B.1.351 viruses to neutralization by 30 mAbs, 20 convalescent plasma, and 22 vaccinee sera. In addition, we created VSV-based SARS-CoV-2 pseudoviruses that contain each of the individual mutations as well as one with all 8 mutations of the B.1.1.7 variant (UKΔ8) and another with all 9 mutations of the B.1.351 variant (SAΔ9). A total of 18 mutant pseudoviruses were made as previously described^{20,21}, and each was found to have a robust titer (Extended Data Fig. 1c) adequate for neutralization studies.

Monoclonal antibodies

We first assayed the neutralizing activity of 12 RBD mAbs against authentic B.1.1.7 and B.1.351 viruses, as compared to the original SARS-CoV-2 strain (WT), in Vero E6 cells as previously described^{20,21}. Three mAbs

¹Aaron Diamond AIDS Research Center, Columbia University Vagelos College of Physicians and Surgeons, New York, NY, USA. ²Department of Microbiology and Immunology, Columbia University Irving Medical Center, New York, NY, USA. ³Vaccine Research Center, National Institutes of Health, Bethesda, MD, USA. ⁴Department of Biochemistry, Columbia University, New York, NY, USA. ⁵Division of Infectious Diseases, Department of Internal Medicine, Columbia University Vagelos College of Physicians and Surgeons, New York, NY, USA. ⁶Regeneron Pharmaceuticals, Inc., Tarrytown, NY, USA. ⁷Zuckerman Mind Brain Behavior Institute, Columbia University, New York, NY, USA. ⁸These authors contributed equally: Pengfei Wang, Manoj S. Nair, Lihong Liu, and Sho Iketani. ✉e-mail: yh3253@cumc.columbia.edu; dh2994@cumc.columbia.edu

target the “inner side”, four target RBM, and five target the “outer side”. The footprints of these mAbs on RBD are shown in Fig. 1a, and their neutralization profiles are shown in Fig. 1b. For neutralization of B.1.1.7, only the activities of 910-30²² and S309⁵ are significantly impaired. For neutralization of B.1.351, however, the activities of 910-30, 2-15²⁰, LY-CoV555 (bamlanivimab)^{1,23}, C121²⁴, and REGN10933 (casirivimab)² are completely or markedly abolished. The four mAbs that target RBM are among the most potent SARS-CoV-2-neutralizing antibodies in clinical use or development. Note that mAbs directed to lower aspects of the “inner side” (2-36²⁰ & COVA1-16^{25,26}) or to the “outer side” retain their activities against B.1.351, including 2-7^{20,27}, REGN10987 (imdevimab)², C135²⁴, and S309 that are in clinical use or development. The results on the neutralization of B.1.1.7 and B.1.351 by these 12 mAbs are summarized in Fig. 2a as fold increase or decrease in IC50 neutralization titers relative to the WT. To understand the specific spike mutations responsible for the observed changes, we also tested the same panel of mAbs against pseudoviruses UKΔ8 and SΔΔ9, as well as those containing only a single mutation found in B.1.1.7 or B.1.351. The results are displayed, among others, in Extended Data Fig. 3 and summarized in Fig. 2a. There is general agreement for results between B.1.1.7 and UKΔ8, as well as between B.1.351 and SΔΔ9. Against B.1.1.7, the decreased activity of 910-30 is mediated by N501Y, whereas the slightly impaired activity of S309 is unexplained. Against B.1.351, the complete loss of activity of 2-15, LY-CoV555, and C121 is mediated by E484K; the complete loss for 910-30 is mediated by K417N; and the marked reduction for REGN10933 is mediated by K417N and E484K, as has been reported²⁸. A structural explanation on how E484K disrupts the binding of 2-15, LY-CoV555, and REGN10933 is presented in Extended Data Fig. 4a.

We also assessed the neutralizing activity of six NTD mAbs against B.1.1.7, B.1.351, and WT viruses. Both B.1.1.7 and B.1.351 are profoundly resistant to neutralization by our antibodies 5-24 and 4-8²⁰, as well as by 4A8²⁹, all of which target the antigenic supersite in NTD¹⁸ (Insert in Fig. 2b). The activities of 2-17, 4-19, and 5-7²⁰ are variably impaired, particularly against B.1.351. To understand the specific mutations responsible for the observed changes, we then tested these mAbs against pseudoviruses containing only a single mutation found in B.1.1.7 or B.1.351 (Extended Data Fig. 3). The results are summarized in Fig. 2a as fold increase or decrease relative to the WT (D614G). It is evident that the resistance of B.1.1.7 to most NTD mAbs is largely conferred by 144del, whereas the resistance of B.1.351 is largely conferred by 242-244del and/or R246I. Amino-acid residues 144, 242-244, and 246 all fall within the NTD supersite^{18,19} (Insert in Fig. 2b; details in Extended Data Fig. 4b).

We next tested the neutralizing activity of 12 additional RBD mAbs, including ones from our own collection (1-20, 4-20, 2-4, 2-43, 2-30, & 2-38)²⁰ as well as CB6 (etesevimab)^{3,6}, COV2-2196 & COV2-2130⁷, B.1.1.7 & B.1.351, and WT are highlighted in Extended Data Fig. 5a, and the detailed findings against the single-mutation pseudoviruses are shown in Extended Data Fig. 3. The fold changes in neutralization IC50 titers relative to the WT are tabulated in Extended Data Fig. 5b. Here, we only comment on results for mAbs in clinical development. The activity of CB6 is rendered inactive against B.1.351 because of K417N. B.1.1.7 and COV2-2130 are essentially unaffected by the new variants; the activities of B.1.1.7 and COV2-2196 are diminished 14.6 fold and 6.3 fold, respectively, against B.1.351 but not against B.1.1.7.

Lastly, we examined, in a single experiment, the neutralizing activity of mAb therapies in clinical use or under clinical investigation against B.1.1.7, B.1.351, and WT viruses, as well as against UKΔ8, SΔΔ9, and WT pseudoviruses. The results for single mAb LY-CoV555 and S309, as well as for combination regimens REGN10933+REGN10987, LY-CoV555+CB6, B.1.1.7+B.1.351, and COV2-2196+COV2-2130, are shown in Extended Data Fig. 6 and summarized in Fig. 2c. Note that LY-CoV555, alone or in combination with CB6, is no longer able to neutralize B.1.351. While REGN10933+REGN10987 and COV2-2196+COV2-2130 are seemingly

unaffected against variant pseudoviruses, there are noticeable decreases in their activity against B.1.351 authentic virus. Although S309 and the B.1.1.7+B.1.351 combination are not significantly impaired, their potencies are noticeably lower (Fig. 2c). These findings suggest that antibody treatment of this virus might need to be modified in localities where B.1.351 and related variants^{13,14} are prevalent, and highlight the importance of combination antibody therapy to address the expanding antigenic diversity of SARS-CoV-2.

Convalescent plasma

We obtained convalescent plasma from 20 patients more than one month after documented SARS-CoV-2 infection in the Spring of 2020. Each plasma sample was then assayed for neutralization against B.1.1.7, B.1.351, and WT viruses. Fig. 3a shows that most (16 of 20) plasma samples lost >2.5-fold neutralizing activity against B.1.351, while maintaining activity against B.1.1.7. Only plasma from P7, P10, P18, and P20 retain neutralizing activities similar to those against the WT. These results are summarized as fold increase or decrease in plasma neutralization ID50 titers in Fig. 3b. Furthermore, the magnitude of the drop in plasma neutralization is better seen in Fig. 3c, showing no loss of activity against B.1.1.7 but substantial loss against B.1.351 (9.4 fold).

Every plasma sample was also tested against each mutant pseudovirus, and those findings are shown in Extended Data Fig. 7 and summarized in Figs. 3b & 3c. Eight samples show >2.5-fold decrease in neutralizing activity against UKΔ8, in contrast to the results for B.1.1.7 neutralization. These discrepant results highlight our previous observation²⁰ that pseudovirus neutralization does not always faithfully recapitulate live virus neutralization. The loss of plasma neutralizing activity against B.1.351 could be largely attributed to E484K (Fig. 3b), which has been shown to attenuate the neutralizing activity of convalescent sera³⁰. Our findings here suggests that this RBM mutation is situated in an immunodominant epitope for most infected persons. It is also interesting to note that cases such as P7, P10, and P18 have neutralizing antibodies that are essentially unperturbed by the multitude of spike mutations found in these two new variants (Fig. 3b). A detailed analysis of their antibody repertoire against the viral spike could be informative.

Vaccinee Sera

Sera were obtained from 12 participants of a Phase 1 clinical trial of Moderna SARS-CoV-2 mRNA-1273 Vaccine⁹ conducted at the NIH. These volunteers received two immunizations with the vaccine (100 µg) on days 0 and 28, and blood was collected on day 43. Additional vaccinee sera were obtained from 10 individuals who received the Pfizer BNT162b2 Covid-19 Vaccine¹⁰ under emergency use authorization at the clinical dose on days 0 and 21. Blood was collected on day 28 or later.

Each vaccinee serum sample was assayed for neutralization against B.1.1.7, B.1.351, and WT viruses. Fig. 4a shows no loss of neutralizing activity against B.1.1.7, whereas every sample lost activity against B.1.351. These results are quantified and tabulated as fold increase or decrease in neutralization ID50 titers in Fig. 4b, and the extent of the decline in neutralization activity is more evident in Fig. 4c. Overall, the neutralizing activity against B.1.1.7 was essentially unchanged, but significantly lower against B.1.351 (12.4 fold, Moderna; 10.3 fold, Pfizer).

Every vaccinee serum was also tested against each mutant pseudovirus, and the results are presented in Extended Data Fig. 8 and summarized in Figs. 4b & 4c. No single mutation in B.1.1.7 has an appreciable impact on the neutralizing activity of vaccinee sera. The loss of neutralizing activity against SΔΔ9 is largely consistent with the loss in B.1.351 live virus neutralization. A major contributor to the neutralization resistance of this variant virus appears to be E484K (Fig. 4b), indicating that this RBM mutation is situated in an immunodominant epitope recognized by all vaccinees studied.

Discussion

Both SARS-CoV-2 variants B.1.1.7 and B.1.351 are raising concerns not only because of their increase transmissibility but also because of their extensive mutations in spike that could lead to antigenic changes detrimental to mAb therapies and vaccine protection. It is of equal concern that another variant known as P.1 or 501Y.V3 is increasing rapidly in Brazil and spreading far beyond^{13,14}. P.1 contains three mutations (K417T, E484K, and N501Y) at the same RBD residues as B.1.351. Much of our findings on B.1.351 would likely be similar for this emergent variant. N501Y is shared among viruses in these three lineages; while this mutation may confer enhanced binding to ACE2³¹, its antigenic impact is limited to a few mAbs (Fig. 2a & Extended Data Fig. 5b), with no pronounced effects on the neutralizing activity of convalescent plasma or vaccinee sera (Figs. 3b & 4b), as others are reporting^{32–34}.

Our findings have relevance to the use of mAb to treat or prevent SARS-CoV-2. Both B.1.1.7 and B.1.351 are resistant to neutralization by mAbs directed to the NTD supersite (Figs. 2a, 2b, & Extended Data Fig. 4b). More importantly, B.1.351 is resistant to a major group of potent mAbs that target the RBM, including three regimens authorized for emergency use (Fig. 2a). LY-CoV555 alone and in combination with CB6 are inactive against B.1.351, and the activity of REGN10933 is impaired (Fig. 1b) while its combination with REGN10987 retains much of the activity (Fig. 2c). Several other mAbs in development are similarly impaired (Figs. 2a, 2c, & Extended Data Fig. 5b) against this variant. Decisions on the use of these mAbs will depend heavily on the local prevalence of B.1.351 or variants with an E484K mutation, thus highlighting the importance of viral genomic surveillance worldwide and proactive development of next-generation antibody therapeutics, including combinations that target antigenically distinct epitopes.

Convalescent plasma from patients infected with SARS-CoV-2 from early in the pandemic show no significant change in neutralizing activity against B.1.1.7, but the diminution against B.1.351 is remarkable (Figs. 3b & 3c). This relative resistance is largely due to E484K, a mutation shared by B.1.351 and P.1^{12–14}. Again, in areas where such viruses are common, one would have a concern about re-infection, as other studies are also suggesting^{35,36}. This apprehension is heightened by the recent observation from the Novavax vaccine trial in South Africa that placebo recipients with prior SARS-CoV-2 infection were not protected against a subsequent exposure to B.1.351^{37,38}. Even more disturbing is the situation in Manaus, Brazil where a second wave of infection due to P.1 is sweeping through a population that was already 76% seropositive due to prior infection in the Spring of 2020³⁹.

As for the ramifications of our findings for the protective efficacy of current SARS-CoV-2 vaccines, the neutralizing activity of vaccinee sera against B.1.1.7 is largely intact and no adverse impact on current vaccines is expected (Fig. 4c), consistent with conclusions being reached by others^{34,40,41}. On the other hand, the loss of 10.3–12.4 fold in activity against B.1.351 is larger than results being reported using mutant pseudoviruses^{34,42,43}. Taken together, the overall findings are worrisome, particularly in light of recent reports that both Novavax and Johnson & Johnson vaccines showed a substantial drop in efficacy in South Africa^{37,38}.

The recent emergence of B.1.1.7, B.1.351, and P.1 marks the beginning of SARS-CoV-2 antigenic drift. This conclusion is supported by data presented herein, illustrating how so many of these spike changes conferred resistance to antibody neutralization, and by studies reporting similar spike mutations selected by antibody pressure in vivo^{44–46}. Mutationally, this virus is traveling in a direction that could ultimately lead to escape from our current therapeutic and prophylactic interventions directed to the viral spike. If the rampant spread of the virus continues and more critical mutations accumulate, then we may be condemned to chasing after the evolving SARS-CoV-2 continually, as we have long done for influenza virus. Such considerations require that we stop virus transmission as quickly as is feasible, by redoubling our mitigation measures and by expediting vaccine rollout.

Online content

Any methods, additional references, Nature Research reporting summaries, source data, extended data, supplementary information, acknowledgements, peer review information; details of author contributions and competing interests; and statements of data and code availability are available at <https://doi.org/10.1038/s41586-021-03398-2>.

1. Chen, P. et al. SARS-CoV-2 Neutralizing Antibody LY-CoV555 in Outpatients with Covid-19. *N Engl J Med* **384**, 229–237 (2021).
2. Hansen, J. et al. Studies in humanized mice and convalescent humans yield a SARS-CoV-2 antibody cocktail. *Science* **369**, 1010–1014 (2020).
3. Gottlieb, R. L. et al. Effect of Bamlanivimab as Monotherapy or in Combination With Etesevimab on Viral Load in Patients With Mild to Moderate COVID-19: A Randomized Clinical Trial. *JAMA* (2021).
4. Ju, B. et al. Human neutralizing antibodies elicited by SARS-CoV-2 infection. *Nature* **584**, 115–119 (2020).
5. Pinto, D. et al. Cross-neutralization of SARS-CoV-2 by a human monoclonal SARS-CoV antibody. *Nature* **583**, 290–295 (2020).
6. Shi, R. et al. A human neutralizing antibody targets the receptor-binding site of SARS-CoV-2. *Nature* **584**, 120–124 (2020).
7. Zost, S. J. et al. Potently neutralizing and protective human antibodies against SARS-CoV-2. *Nature* **584**, 443–449 (2020).
8. Krammer, F. SARS-CoV-2 vaccines in development. *Nature* **586**, 516–527 (2020).
9. Anderson, E. J. et al. Safety and Immunogenicity of SARS-CoV-2 mRNA-1273 Vaccine in Older Adults. *N Engl J Med* **383**, 2427–2438 (2020).
10. Polack, F. P. et al. Safety and Efficacy of the BNT162b2 mRNA Covid-19 Vaccine. *N Engl J Med* **383**, 2603–2615 (2020).
11. Rambaut, A. et al. Preliminary genomic characterisation of an emergent SARS-CoV-2 lineage in the UK defined by a novel set of spike mutations. <https://virological.org/t/preliminary-genomic-characterisation-of-an-emergent-sars-cov-2-lineage-in-the-uk-defined-by-a-novel-set-of-spike-mutations/563>. (2020).
12. Tegally, H. et al. Emergence and rapid spread of a new severe acute respiratory syndrome-related coronavirus 2 (SARS-CoV-2) lineage with multiple spike mutations in South Africa. *medRxiv*, 2020.2012.2021.20248640 (2020).
13. Faria, N. R. et al. Genomic characterisation of an emergent SARS-CoV-2 lineage in Manaus: preliminary findings. <https://virological.org/t/genomic-characterisation-of-an-emergent-sars-cov-2-lineage-in-manauas-preliminary-findings/586>. (2021).
14. Naveca F, et al. Phylogenetic relationship of SARS-CoV-2 sequences from Amazonas with emerging Brazilian variants harboring mutations E484K and N501Y in the Spike protein. <https://virological.org/t/phylogenetic-relationship-of-sars-cov-2-sequences-from-amazonas-with-emerging-brazilian-variants-harboring-mutations-e484k-and-n501y-in-the-spike-protein/585>. (2021).
15. Korber, B. et al. Tracking Changes in SARS-CoV-2 Spike: Evidence that D614G Increases Infectivity of the COVID-19 Virus. *Cell* **182**, 812–827 e819 (2020).
16. Hou, Y. J. et al. SARS-CoV-2 D614G variant exhibits efficient replication ex vivo and transmission in vivo. *Science* **370**, 1464–1468 (2020).
17. Davies, N. G. et al. Increased hazard of death in community-tested cases of SARS-CoV-2 Variant of Concern 202012/01. *medRxiv*, 2021.2002.2001.21250959 (2021).
18. Cerutti, G. et al. Potent SARS-CoV-2 Neutralizing Antibodies Directed Against Spike N-Terminal Domain Target a Single Supersite. *bioRxiv*, 2021.2001.2010.426120 (2021).
19. McCallum, M. et al. N-terminal domain antigenic mapping reveals a site of vulnerability for SARS-CoV-2. *bioRxiv*, 2021.2001.2014.426475 (2021).
20. Liu, L. et al. Potent neutralizing antibodies against multiple epitopes on SARS-CoV-2 spike. *Nature* **584**, 450–456 (2020).
21. Wang, P. et al. SARS-CoV-2 neutralizing antibody responses are more robust in patients with severe disease. *Emerg Microbes Infect* **9**, 2091–2093 (2020).
22. Banach, B. B. et al. Paired heavy and light chain signatures contribute to potent SARS-CoV-2 neutralization in public antibody responses. *bioRxiv*, 2020.2012.2031.424987 (2021).
23. Jones, B. E. et al. LY-CoV555, a rapidly isolated potent neutralizing antibody, provides protection in a non-human primate model of SARS-CoV-2 infection. *bioRxiv* (2020).
24. Robbiani, D. F. et al. Convergent antibody responses to SARS-CoV-2 in convalescent individuals. *Nature* **584**, 437–442 (2020).
25. Brouwer, P. J. M. et al. Potent neutralizing antibodies from COVID-19 patients define multiple targets of vulnerability. *Science* **369**, 643–+ (2020).
26. Liu, H. et al. Cross-Neutralization of a SARS-CoV-2 Antibody to a Functionally Conserved Site Is Mediated by Avidity. *Immunity* **53**, 1272–1280 e1275 (2020).
27. Cerutti, G. et al. Structural Basis for Accommodation of Emerging B.1.351 and B.1.1.7 Variants by Two Potent SARS-CoV-2 Neutralizing Antibodies. *bioRxiv*, 2021.2002.2021.432168 (2021).
28. Starr, T. N. et al. Prospective mapping of viral mutations that escape antibodies used to treat COVID-19. *Science*, eabf9302 (2021).
29. Chi, X. et al. A neutralizing human antibody binds to the N-terminal domain of the Spike protein of SARS-CoV-2. *Science* **369**, 650–655 (2020).
30. Greaney, A. J. et al. Comprehensive mapping of mutations to the SARS-CoV-2 receptor-binding domain that affect recognition by polyclonal human serum antibodies. *bioRxiv*, 2020.2012.2031.425021 (2021).
31. Starr, T. N. et al. Deep Mutational Scanning of SARS-CoV-2 Receptor Binding Domain Reveals Constraints on Folding and ACE2 Binding. *Cell* **182**, 1295–1310 e1220 (2020).
32. Xie, X. et al. Neutralization of SARS-CoV-2 spike 69/70 deletion, E484K and N501Y variants by BNT162b2 vaccine-elicited sera. *Nature Medicine* (2021).

33. Rees-Spear, C. *et al.* The impact of Spike mutations on SARS-CoV-2 neutralization. *bioRxiv*, 2021.2001.2015.426849 (2021).
34. Wu, K. *et al.* mRNA-1273 vaccine induces neutralizing antibodies against spike mutants from global SARS-CoV-2 variants. *bioRxiv*, 2021.2001.2025.427948 (2021).
35. Cele, S. *et al.* Escape of SARS-CoV-2 501Y.V2 variants from neutralization by convalescent plasma. *medRxiv*, 2021.2001.2026.21250224 (2021).
36. Wibmer, C. K. *et al.* SARS-CoV-2 501Y.V2 escapes neutralization by South African COVID-19 donor plasma. *bioRxiv*, 2021.2001.2018.427166 (2021).
37. Wadman, M. & Cohen, J. Novavax vaccine delivers 89% efficacy against COVID-19 in U.K.—but is less potent in South Africa, <https://www.sciencemag.org/news/2021/01/novavax-vaccine-delivers-89-efficacy-against-covid-19-uk-less-potent-south-africa>. (2021).
38. Callaway, E. & Mallapaty, S. Novavax offers first evidence that COVID vaccines protect people against variants. <https://www.nature.com/articles/d41586-021-00268-9>. (2021).
39. Sabino, E. C. *et al.* Resurgence of COVID-19 in Manaus, Brazil, despite high seroprevalence. *Lancet* **397**, 452–455 (2021).
40. Collier, D. *et al.* Impact of SARS-CoV-2 B.1.1.7 Spike variant on neutralisation potency of sera from individuals vaccinated with Pfizer vaccine BNT162b2. *medRxiv*, 2021.2001.2019.21249840 (2021).
41. Muik, A. *et al.* Neutralization of SARS-CoV-2 lineage B.1.1.7 pseudovirus by BNT162b2 vaccine-elicited human sera. *bioRxiv*, 2021.2001.2018.426984 (2021).
42. Wang, Z. *et al.* mRNA vaccine-elicited antibodies to SARS-CoV-2 and circulating variants. *Nature* (2021).
43. Tada, T. *et al.* Neutralization of viruses with European, South African, and United States SARS-CoV-2 variant spike proteins by convalescent sera and BNT162b2 mRNA vaccine-elicited antibodies. *bioRxiv*, 2021.2002.2005.430003 (2021).
44. Kemp, S. A. *et al.* SARS-CoV-2 evolution during treatment of chronic infection. *Nature* (2021).
45. McCarthy, K. R. *et al.* Recurrent deletions in the SARS-CoV-2 spike glycoprotein drive antibody escape. *Science*, eabf6950 (2021).
46. Choi, B. *et al.* Persistence and Evolution of SARS-CoV-2 in an Immunocompromised Host. *N Engl J Med* **383**, 2291–2293 (2020).

Publisher's note Springer Nature remains neutral with regard to jurisdictional claims in published maps and institutional affiliations.

© The Author(s), under exclusive licence to Springer Nature Limited 2021

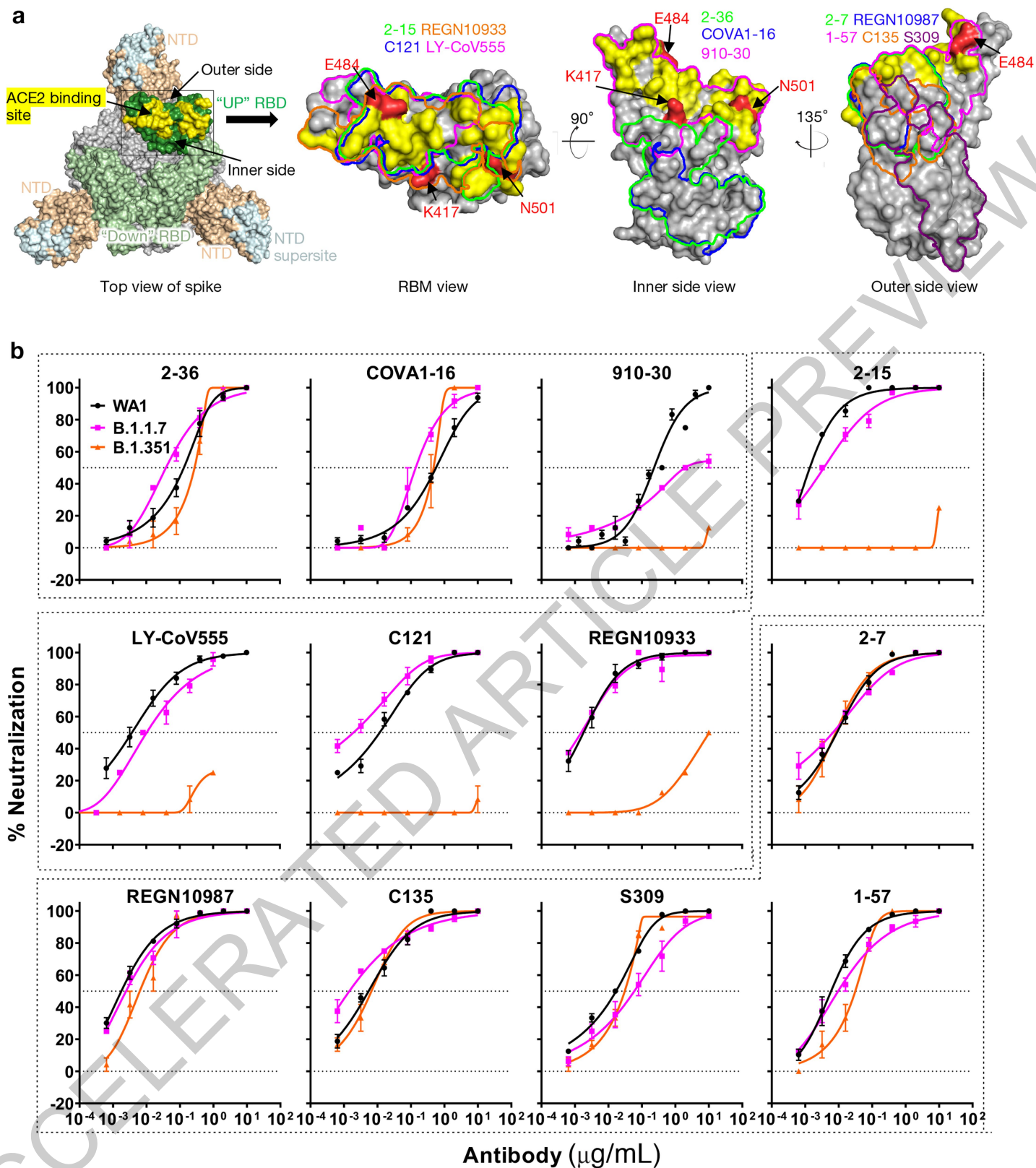


Fig. 1 | Susceptibility of B.1.1.7 and B.1.351 to neutralization by mAbs.

a, Footprints of neutralizing mAbs on the RBD. Left panel, top view of SARS-CoV-2 spike with one RBD in the “up” conformation (pdb: 6zgg). RBD and NTD are colored green and peach, respectively. The positions of ‘inner’ and ‘outer’ sides are indicated on the “up” RBD with the ACE2-binding site colored

yellow. The three panels to the right show the antibody footprints on RBD.

b, Neutralization of B.1.1.7, B.1.351, and WT viruses by select RBD mAbs. Data are mean \pm SEM of technical triplicates, and represent one of two independent experiments. Neutralization by negative control mAbs is shown in Extended Data Fig. 2a.

a

Fold Change of IC50 from WT	RBD-directed mAbs												NTD-directed mAbs						
	Inner side			RBM					Outer side				Supersite			Others			
	2-36	COVA1-16	910-30	2-15	LY-CoV555	C121	REGN10933	2-7	REGN10987	C135	S309	1-57	5-24	4-8	4A8	2-17	4-19	5-7	
UK	B.1.1.17	3.4	3.4	-10.3	-3.0	-2.8	4.0	1.0	1.5	1.0	3.0	-4.0	-1.5	-330.2	<-1000	<-1000	-42.6	-29.2	-7.5
	UKΔ8	1.2	1.3	-14.0	2.2	1.7	2.3	2.5	1.4	2.1	-1.4	-3.1	2.1	<-1000	<-1000	<-1000	-121.2	-20.5	-11.9
	69-70del	-1.0	1.1	2.7	1.2	1.1	1.7	1.3	-1.2	1.2	1.8	-1.6	1.1	1.1	1.1	1.5	-1.1	-3.6	-4.0
	144del	1.5	-1.3	2.3	1.3	1.1	1.7	1.3	1.2	-1.4	1.4	1.4	1.1	<-1000	<-1000	<-1000	-80.7	1.6	-3.7
	N501Y	-1.2	-1.4	-12.7	1.5	-1.0	1.5	-1.4	-1.0	1.3	1.2	1.2	3.6	-2.9	-6.7	MPI↓	-12.0	-1.4	-3.2
	A570D	4.1	1.9	6.7	1.4	1.7	1.7	4.7	-2.3	-1.6	1.1	-1.2	2.2	1.1	-15.1	-2.9	-4.8	-1.9	-2.2
	P681H	2.0	1.5	2.5	3.1	2.3	-1.0	1.6	-1.4	-1.9	1.3	-1.2	2.9	-1.5	-2.8	1.1	-4.7	-1.2	1.8
	T716I	4.3	3.9	3.9	3.1	3.5	2.0	3.6	-1.1	-1.6	1.2	-1.6	2.9	-3.5	-5.5	MPI↓	-2.6	1.2	-1.0
	S982A	-3.9	-3.0	-2.4	1.1	-2.0	1.4	-2.3	-2.2	-1.2	1.6	-1.0	-1.5	-1.1	-1.1	-2.9	-4.3	1.2	-1.3
	D1118H	-1.1	-3.1	1.0	1.2	1.0	1.7	-1.3	-1.4	-1.7	1.2	1.5	1.1	-1.3	-3.1	1.4	-1.1	-1.1	-1.8
SA	B.1.351	-2.1	1.0	-456.6	<-1000	<-1000	<-1000	<-1000	1.1	-3.5	1.0	-2.2	-5.2	<-1000	<-1000	<-1000	-456.4	-595.2	-84.8
	SAΔ9	-2.0	1.3	<-1000	<-1000	<-1000	<-1000	-58.8	1.3	1.8	1.2	1.3	3.3	<-1000	<-1000	<-1000	-406.6	<-1000	-18.1
	L18F	1.5	1.9	2.8	3.0	1.0	1.8	1.4	-1.4	-1.8	1.1	1.2	-1.6	-2.2	1.3	MPI↓	-107.2	<-1000	-8.9
	D80A	-1.4	1.2	2.1	2.0	1.5	2.0	1.4	-2.2	-2.2	1.0	2.2	-2.7	2.3	2.0	-1.0	-2.0	<-1000	-9.8
	D215G	1.9	1.6	1.5	1.8	1.5	2.1	1.5	-1.8	-2.1	-1.2	1.0	2.2	-1.1	-1.8	-2.3	-6.0	1.1	1.1
	242-244del	-1.4	1.2	-1.2	1.4	-1.1	1.1	1.0	-1.2	-3.2	1.8	1.2	-1.3	<-1000	<-1000	<-1000	<-1000	<-1000	-20.7
	R246I	1.3	1.7	2.2	2.4	1.4	2.1	2.2	1.4	-2.1	1.1	2.3	1.7	<-1000	<-1000	<-1000	-2.8	<-1000	-9.2
	K417N	3.2	3.3	<-1000	3.3	8.4	1.2	-13.1	2.1	-1.2	2.9	1.6	7.8	2.9	-1.6	1.7	-1.5	1.2	-1.2
	E484K	-1.2	-1.0	4.3	<-1000	<-1000	<-1000	-10.5	-3.4	-1.1	2.3	2.5	-1.1	-1.6	-3.2	MPI↓	-2.8	-1.1	-1.4
	N501Y	-1.2	-1.4	-12.7	1.5	-1.0	1.5	-1.4	-1.0	1.3	1.2	1.2	3.6	-2.9	-6.7	MPI↓	-12.0	-1.4	-3.2
	A701V	1.9	1.4	2.1	2.8	2.0	1.6	2.3	-1.8	-2.6	1.5	1.1	2.5	-3.3	-2.0	MPI↓	-3.3	-1.2	-1.3

Red: resistance >3 fold; Green: sensitization >3 fold

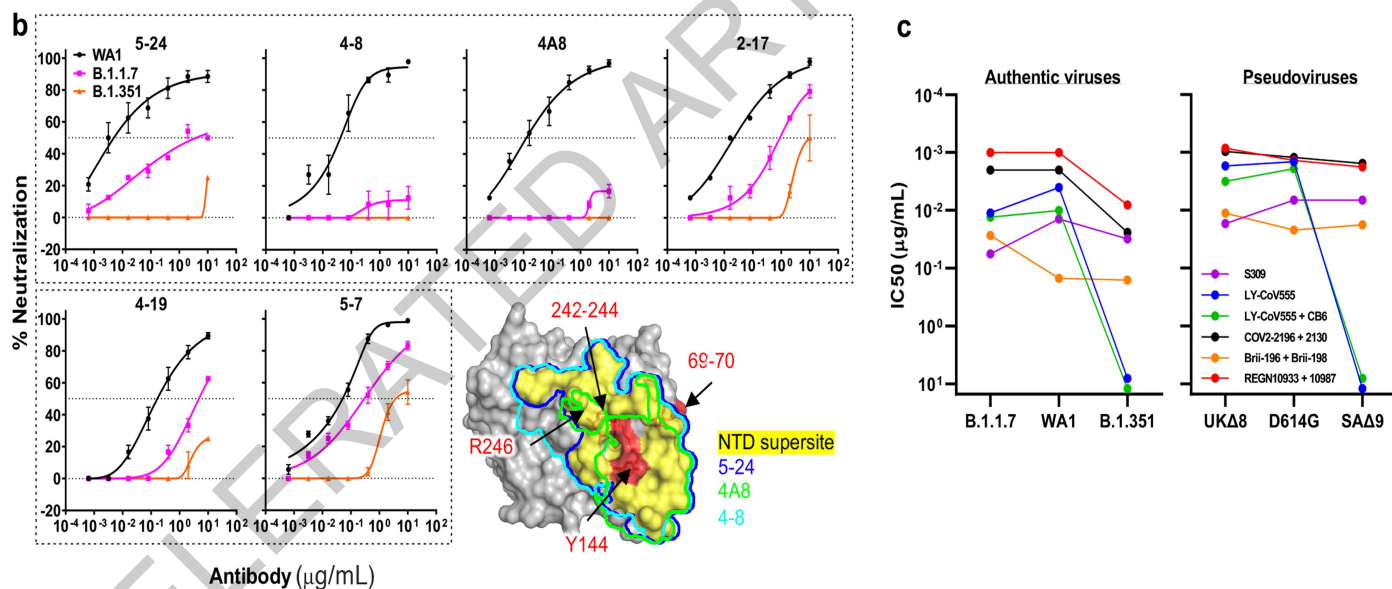
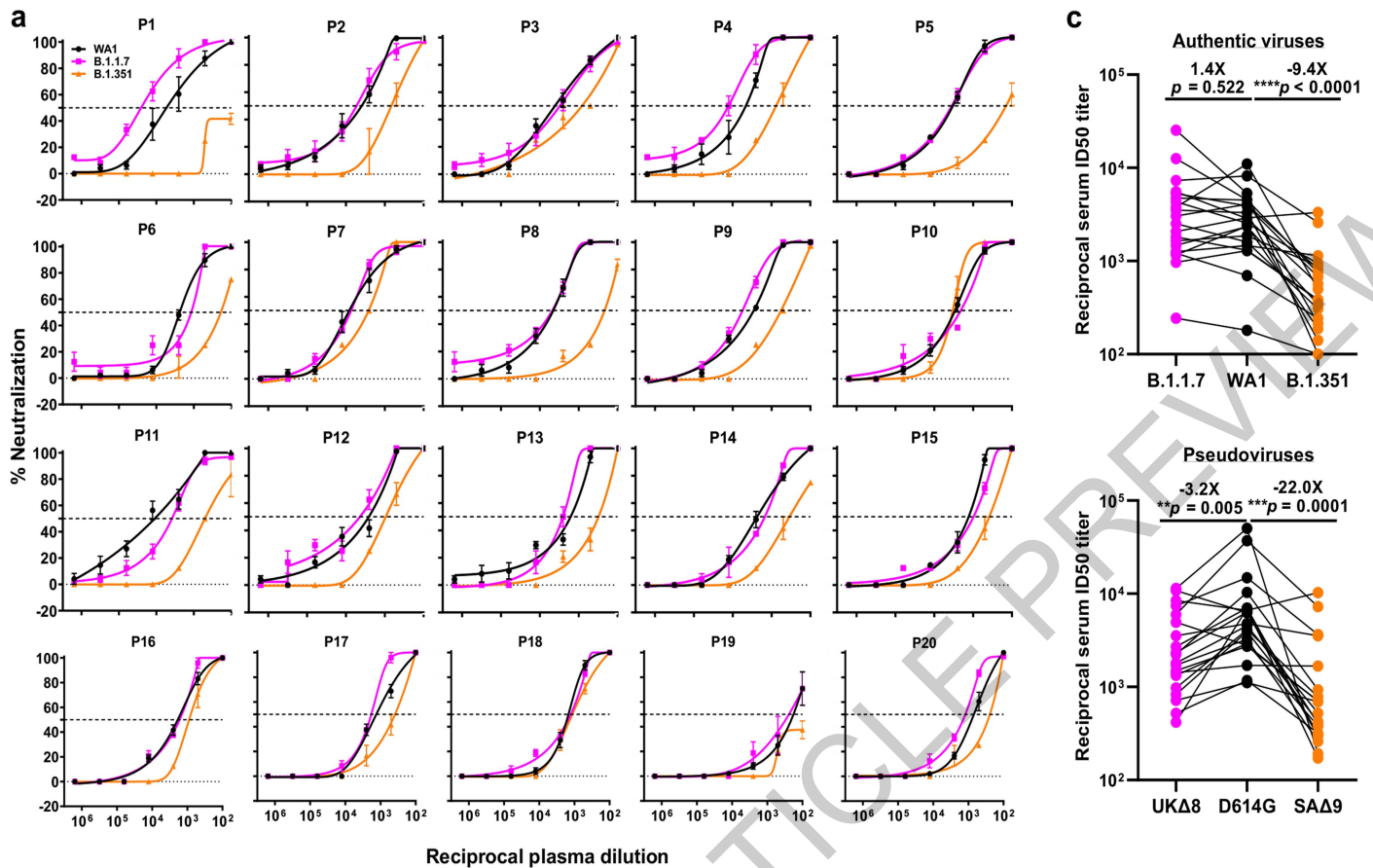


Fig. 2 | Susceptibility of B.1.1.7 and B.1.351 to neutralization by mAbs (continued). **a**, Fold increase or decrease in IC50 of neutralizing mAbs against B.1.1.7 and B.1.351, as well as UKΔ8, SAΔ9, and single-mutation pseudoviruses, relative to WT, presented as a heatmap with darker colors implying greater change. MPI↓ denotes that maximum percent inhibition is substantially reduced, confounding IC50 calculations. **b**, Neutralization of B.1.1.7, B.1.351,

and WT viruses by NTD-directed mAbs, the footprints of which are delineated by the color tracings in the insert. Data are mean ± SEM of technical triplicates, and represent one of two independent experiments. **c**, Changes in neutralization IC50 of authorized or investigational therapeutic mAbs against B.1.1.7, B.1.351, WT (WA1) viruses as well as UKΔ8, SAΔ9, and WT (D614G) pseudoviruses.



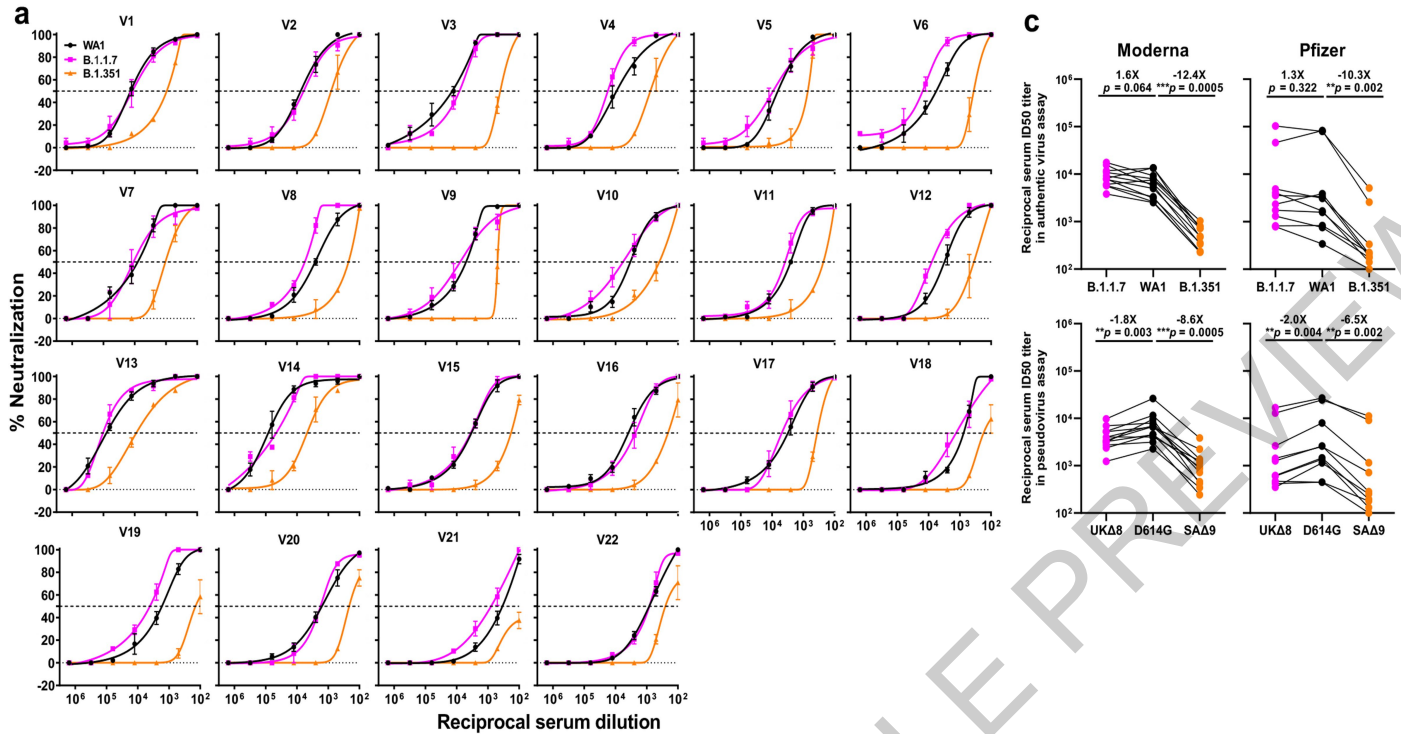
b

Fold change of ID50 from WT	Convalescent plasma																			
	P1	P2	P3	P4	P5	P6	P7	P8	P9	P10	P11	P12	P13	P14	P15	P16	P17	P18	P19	P20
B.1.1.7	4.8	1.4	-1.3	2.8	1.1	-2.0	-1.1	1.1	1.9	-1.4	-2.9	1.7	1.6	-1.6	-1.3	-1.1	1.4	-1.2	1.4	1.7
UKΔ8	-4.4	-6.2	-2.0	-4.6	-2.6	-16.7	1.3	-2.7	1.7	-1.4	-2.5	-4.2	-4.7	-1.9	-2.2	1.8	-1.8	-1.2	-2.3	-1.5
69-70del	-1.9	-1.8	2.3	1.8	-1.8	-1.5	1.4	-1.3	1.2	1.6	-1.9	1.7	-2.0	1.5	1.2	-1.1	-1.8	1.0	-1.1	1.2
144del	1.3	2.8	1.4	2.6	-1.4	-4.5	-1.1	-1.5	1.0	-1.1	-4.5	-1.1	-2.2	-1.4	1.1	-1.6	-2.0	-1.5	-2.0	-1.4
N501Y	-1.6	-2.3	1.9	1.0	-1.1	-3.6	1.0	-2.4	1.5	1.2	-2.0	-2.1	-3.1	-1.3	-1.7	-1.3	-1.5	1.0	-1.3	1.4
A570D	1.0	4.3	1.9	5.1	-1.1	-3.2	1.4	-1.6	1.5	1.4	-2.7	1.4	-3.1	1.1	-1.1	-1.1	-1.2	-1.1	-1.0	-1.0
P681H	-1.8	-1.5	-1.6	1.1	-1.9	-2.3	1.0	-1.7	1.0	1.3	-2.6	-1.5	-4.1	1.1	-1.4	-1.3	-1.8	-1.3	-1.9	1.0
T716I	-1.1	1.3	1.9	1.9	1.6	-3.7	-1.4	-2.5	-1.1	-1.0	-2.8	-1.4	-6.4	1.0	-2.0	-1.9	-2.3	-2.0	-1.8	-1.4
S982A	-5.0	-9.3	1.2	-1.5	-2.5	-2.8	1.0	-3.0	1.2	1.1	-2.2	-2.7	-3.7	-1.4	-1.4	-1.1	-2.0	1.2	-2.4	-1.7
D1118H	-2.1	-1.9	2.0	1.1	-1.5	-2.6	1.0	-3.1	1.2	-1.1	-2.6	-1.4	-3.0	1.0	-1.7	-1.3	-1.7	-1.1	-1.5	1.0
B.1.351	-53.3	-5.8	-5.0	-6.1	-23.4	-12.5	-3.2	-20.9	-5.1	1.1	-21.9	-2.7	-5.2	-6.8	-3.4	-2.1	-3.4	-1.3	-1.8	-2.9
SAA9	-260.6	-5.1	-4.1	-11.1	-22.8	-40.4	1.6	-21.4	-15.5	-1.4	-8.7	-5.2	-9.3	-12.5	-7.7	-4.0	-3.9	1.0	-3.7	-1.6
L18F	-1.2	1.0	1.9	3.0	-1.9	1.7	1.5	-1.1	1.5	1.1	1.9	-1.1	-1.5	1.3	-1.2	2.1	1.3	-1.1	1.8	1.0
D80A	1.0	-2.3	-1.4	-1.0	-1.5	-2.8	1.8	-2.3	2.2	1.5	-1.8	1.0	-2.0	2.2	-1.3	2.0	1.4	4.2	-1.2	1.3
D215G	-1.9	-2.3	1.0	1.3	-1.8	-4.4	1.1	-3.1	1.3	-1.5	-3.3	-2.2	-4.5	-2.4	-2.6	-1.4	-2.9	-1.6	-2.3	-2.0
242-244del	-1.1	-2.6	-2.0	-1.5	2.1	-9.3	-1.3	-4.6	2.3	2.4	-2.2	-2.6	-6.8	-1.3	-3.0	-1.2	-3.1	-2.6	-2.1	-1.5
R246I	1.4	-1.2	1.3	1.3	-1.8	-4.0	-1.4	-1.1	1.1	1.3	-4.9	-1.1	-2.1	-1.0	-1.2	-1.3	-1.8	-1.1	-1.8	1.5
K417N	-1.3	1.4	6.6	2.5	-1.1	-2.0	1.8	1.0	1.8	1.2	-1.6	-1.4	-2.1	1.8	-1.2	1.3	-1.1	1.2	-1.2	1.5
E484K	-25.4	-4.7	-1.3	-2.6	-7.6	-9.6	-1.6	-10.8	-9.1	-1.3	-8.1	-3.5	-9.8	-2.3	-6.3	-4.3	-3.3	-1.5	-4.0	-3.5
N501Y	-1.6	-2.3	1.9	1.0	-1.1	-3.6	1.0	-2.4	1.5	1.2	-2.0	-2.1	-3.1	-1.3	-1.7	-1.3	-1.5	-1.0	-1.3	1.4
A701V	-1.3	-3.8	-1.1	-1.2	-1.9	-2.3	-1.0	-2.1	1.4	1.1	-2.9	-1.5	-2.3	-1.1	-1.8	-1.7	-1.7	-1.7	-1.9	-1.1

Red: resistance >2.5 fold; Green: sensitization >2.5 fold

Fig. 3 | B.1.351 is more resistant to neutralization by convalescent plasma from patients. a, Neutralization results for 20 convalescent plasma samples (P1-P20) against B.1.1.7, B.1.351, and WT viruses. Data represent mean ± SEM of technical triplicates. Neutralization by healthy donor plasma is shown in Extended Data Fig. 2b. **b**, Fold increase or decrease in neutralization ID50 of B.1.1.7 and B.1.351, as well as UKΔ8, SAA9, and single-mutation pseudoviruses,

relative to the WT presented as a heatmap with darker colors implying greater change. **c**, Change in reciprocal plasma neutralization ID50 values of convalescent plasma against B.1.1.7 and B.1.351, as well as UKΔ8 and SAA9, relative to the WT. Mean fold changes in ID50 values relative to the WT are written above the *p* values. Statistical analysis was performed using a Wilcoxon matched-pairs signed rank test. Two-tailed *p*-values are reported.



b	Fold change of ID50 from WT	Moderna vaccinee sera												Pfizer vaccinee sera									
		V1	V2	V3	V4	V5	V6	V7	V8	V9	V10	V11	V12	V13	V14	V15	V16	V17	V18	V19	V20	V21	V22
UK	B.1.1.7	-1.1	-1.2	-1.7	1.9	1.5	2.7	1.4	2.1	1.5	1.7	1.5	2.5	1.3	-1.8	1.1	-1.7	1.6	1.7	2.4	1.1	2.3	-1.0
	UKA8	-2.7	-2.2	-3.0	-1.2	-1.7	-1.9	-1.2	-1.9	-1.4	1.0	-1.2	-1.8	-1.6	-1.9	-2.1	-1.8	1.1	-2.4	-2.3	-3.2	-1.1	1.1
	69-70del	1.4	1.4	-1.3	1.2	-1.3	-1.1	1.9	1.1	1.5	-1.4	1.3	1.3	-1.4	1.3	-1.0	-1.0	-1.5	-1.3	1.3	1.3	-1.4	2.1
	144del	-1.1	-1.2	-1.4	2.1	-1.2	-1.2	-1.1	-1.2	-1.2	-1.1	1.1	-1.3	-1.2	-1.7	-1.2	-1.2	-1.3	1.1	-1.2	-1.6	1.1	-1.3
	N501Y	1.5	1.1	-1.8	1.6	-2.0	1.9	2.2	-2.0	-1.2	4.6	2.9	-1.2	-1.2	1.2	-2.1	-1.6	-1.6	-1.5	-1.1	-2.4	-1.4	1.0
	A570D	1.4	2.2	1.2	2.4	1.7	1.6	2.2	1.5	1.0	1.5	1.4	1.6	1.2	1.5	1.5	2.6	1.2	1.3	1.8	1.1	-1.2	1.4
	P681H	2.2	1.2	-1.7	-1.5	-1.5	1.0	1.1	-1.4	1.0	-1.1	1.1	1.1	1.2	1.2	-1.3	1.1	-1.1	-1.1	-1.0	-2.1	-1.3	-1.0
	T716I	1.1	-1.1	-1.1	1.6	1.3	1.3	1.8	1.1	1.0	1.6	1.2	1.4	1.7	1.4	1.3	1.1	1.1	1.3	1.1	1.6	1.1	1.1
	S982A	-2.3	-1.5	-2.6	-1.8	-2.0	-1.6	-1.3	-2.5	-1.7	-1.5	-1.5	-1.5	-1.2	-1.6	-1.6	-1.7	-1.5	-1.9	-1.6	-2.4	-2.0	-1.3
D1118H	-1.2	1.1	-1.2	-1.4	1.1	1.0	1.0	-1.5	-1.2	-1.1	1.0	1.1	-1.2	-1.2	-1.6	-1.6	-1.2	-1.5	-1.2	-1.3	-1.7	-1.3	
SA	B.1.351	-14.4	-9.4	-28.8	-12.1	-8.7	-17.0	-7.7	-11.6	-10.2	-8.4	-11.1	-8.8	-9.0	-17.5	-18.4	-18.5	-9.3	-4.3	-11.9	-7.4	<-3.4	-3.7
	SAA9	-6.9	-8.4	-22.7	-11.0	-6.1	-7.7	-2.9	-10.0	-4.8	-3.2	-13.0	-6.6	-3.0	-2.2	-9.2	-3.5	-2.5	-7.5	-10.4	-4.5	<-4.5	-2.5
	L18F	1.9	1.0	-1.8	-1.1	-1.3	1.0	3.3	-1.5	1.0	1.2	1.8	1.0	1.2	-1.3	1.2	1.2	1.0	-1.4	1.4	-1.4	-1.5	1.4
	D80A	1.2	1.5	-1.1	2.1	1.1	1.5	1.8	-1.5	1.4	3.0	1.3	1.1	1.8	1.0	1.2	1.4	-1.5	-1.8	1.0	-1.8	-1.3	1.1
	D215G	-1.3	1.1	1.1	-1.2	1.3	1.2	-1.1	-2.9	-1.1	2.7	1.1	-1.3	-1.1	1.1	-1.8	-2.0	-1.2	-1.8	-1.3	1.0	-1.2	1.1
	242-244del	-3.8	1.0	-1.3	-1.8	-1.7	-1.3	-1.7	-1.7	-1.4	-1.5	-1.6	-1.6	-1.4	-1.9	-1.4	-1.3	1.5	1.1	-1.3	-2.6	-1.6	-1.8
	R246I	-1.6	1.1	-2.0	-1.1	-1.7	-1.2	1.1	-2.1	-1.3	-1.1	1.0	-1.7	-1.5	-1.2	1.6	1.0	1.3	2.0	2.9	-4.0	1.0	-1.1
	K417N	1.6	1.4	-1.1	1.0	1.0	-1.2	1.7	-1.3	1.1	1.4	-1.3	1.5	1.4	1.8	1.2	1.4	-1.5	1.9	2.0	1.0	-1.8	1.6
	E484K	-3.0	-2.3	-3.9	-4.0	-1.4	-2.8	-1.3	-3.3	-2.2	-2.6	-3.2	-1.8	-1.9	-2.7	-2.1	-1.6	-2.9	-11.3	-3.3	-3.2	-3.1	-1.8
	N501Y	1.5	1.1	-1.8	1.6	-2.0	1.9	2.2	-2.0	-1.2	4.6	2.9	-1.2	-1.2	1.2	-2.1	-1.6	-1.6	-1.5	-1.1	-2.4	-1.4	1.0
A701V	-1.1	-1.2	-1.9	-2.2	-1.7	-1.6	-1.4	-1.7	+1.2	1.1	2.1	-1.1	-1.2	-1.3	-1.2	-1.1	-2.1	-1.5	-1.4	1.1	-2.2	-1.5	

Red: resistance >2.5 fold; Green: sensitization >2.5 fold

Fig. 4 | B.1.351 is more resistant to neutralization by vaccinee sera. **a**, Neutralization profiles for 22 serum samples obtained from persons who received SARS-CoV-2 vaccine made by Moderna (V1-V12) or Pfizer (V13-V22) against B.1.1.7, B.1.351, and WT viruses. Data are mean ± SEM of technical triplicates, and represent one of two independent experiments. **b**, Fold change in serum neutralization ID50 of B.1.1.7 and B.1.351, as well as UKA8, SAA9, and

single-mutation pseudoviruses, relative to the WT, presented as a heatmap with darker colors implying greater change. **c**, Change in reciprocal serum ID50 values for Moderna and Pfizer vaccinees against B.1.1.7 and B.1.351, as well as UKA8 and SAA9, relative to the WT. Mean fold change in ID50 relative to the WT is written above the *p* values. Statistical analysis was performed using a Wilcoxon matched-pairs signed rank test. Two-tailed *p*-values are reported.

Methods

Patients and vaccines

Plasma samples were obtained from patients (age 34–79; mean 54) convalescing from documented SARS-CoV-2 infection approximately one month after recovery or later. These cases were enrolled into an observational cohort study of convalescent patients followed at the Columbia University Irving Medical Center (CUIMC) starting in the Spring of 2020. The study protocol was approved by the CUIMC Institutional Review Board (IRB), and all participants provided written informed consent. From their documented clinical profiles, plasma samples from ten with severe Covid-19 were selected, along with plasma from 10 with non-severe infection, for this study. Sera were obtained from 12 participants in a Phase I clinical trial of Moderna SARS-CoV-2 mRNA-1273 Vaccine conducted at the NIH, under a NIH IRB-approved protocol⁹. Sera were also obtained from 10 individuals followed in a CUIMC IRB-approved protocol to assess immunological responses to SARS-CoV-2 who received the Pfizer BNT162b2 Covid-19 Vaccine as a part of the emergency use authorization.

Monoclonal antibodies

Monoclonal antibodies tested in this study were constructed and produced at Columbia University as previously described²⁰, except REGN10933, REGN10987, REGN10985, COV2-2196, and COV2-2130 were provided by Regeneron Pharmaceuticals, Inc., Brie-196 and Brie-198 were provided by Brie Biosciences, and CB6 was provided by B.Z. and P.D.K.

Authentic SARS-CoV-2 Microplate Neutralization

The SARS-CoV-2 viruses USA-WA1/2020 (WA1), USA/CA_CDC_5574/2020 (B.1.1.7), and hCoV-19/South Africa/KRISP-EC-K005321/2020 (B.1.351) were obtained from BEI Resources (NIAID, NIH) and propagated for one passage using Vero-E6 cells. Virus infectious titer was determined by an end-point dilution and cytopathic effect (CPE) assay on Vero-E6 cells as described previously²⁰.

An end-point dilution microplate neutralization assay was performed to measure the neutralization activity of convalescent plasma samples, vaccineesera, and purified mAbs. In brief, plasma and serum samples were subjected to successive 5-fold dilutions starting from 1:100. Similarly, most mAbs were serially diluted (5-fold dilutions) starting at 10 µg/mL. Some clinical antibodies were tested from starting concentrations of 1 µg/mL. Triplicates of each dilution were incubated with SARS-CoV-2 at an MOI of 0.1 in EMEM with 7.5% inactivated fetal calf serum (FCS) for 1 hour at 37 °C. Post incubation, the virus-antibody mixture was transferred onto a monolayer of Vero-E6 cells grown overnight. The cells were incubated with the mixture for ~70 hours. Cytopathic effect (CPE) of viral infection was visually scored for each well in a blinded fashion by two independent observers. The results were then converted into percentage neutralization at a given sample dilution or mAb concentration, and the averages ± SEM were plotted using a five-parameter dose-response curve in GraphPad Prism v8.4.

Construction and production of variant pseudoviruses

The original pCMV3-SARS-CoV-2-spike plasmid was kindly provided by Dr. Peihui Wang of Shandong University in China. Plasmids encoding for D614G variant, all the single-mutation variants found in B.1.1.7 or B.1.351, 8-mutation-combination variant (UKΔ8) and 9-mutation-combination variant (SAΔ9) were generated by Quikchange II XL site-directed mutagenesis kit (Agilent). Recombinant

Indiana VSV (rVSV) expressing different SARS-CoV-2 spike variants were generated as previously described^{20,21}. HEK293T cells were grown to 80% confluency before transfection with the spike gene using Lipofectamine 3000 (Invitrogen). Cells were cultured overnight at 37 °C with 5% CO₂, and VSV-G pseudo-typed ΔG-luciferase (G*ΔG-luciferase, Kerafast) was used to infect the cells in DMEM at an MOI of 3 for 2 hours before washing the cells with 1X DPBS three times. The next day, the transfection supernatant was harvested and clarified by centrifugation at 300 g for 10 min. Each viral stock was then incubated with 20% II hybridoma (anti-VSV-G, ATCC: CRL-2700) supernatant for 1 hour at 37 °C to neutralize contaminating VSV-G pseudo-typed ΔG-luciferase virus before measuring titers and making aliquots to be stored at –80 °C.

Pseudovirus neutralization assays

Neutralization assays were performed by incubating pseudoviruses with serial dilutions of mAbs or heat-inactivated plasma or sera, and scored by the reduction in luciferase gene expression^{20,21}. In brief, Vero E6 cells were seeded in a 96-well plate at a concentration of 2 × 10⁴ cells per well. Pseudoviruses were incubated the next day with serial dilutions of the test samples in triplicate for 30 minutes at 37 °C. The mixture was added to cultured cells and incubated for an additional 24 hours. The luminescence was measured by Luciferase Assay System (Promega). IC₅₀ was defined as the dilution at which the relative light units were reduced by 50% compared to the virus control wells (virus + cells) after subtraction of the background in the control groups with cells only. The IC₅₀ values were calculated using non-linear regression in GraphPad Prism.

Reporting summary

Further information on research design is available in the Nature Research Reporting Summary linked to this paper.

Data availability

Materials used in this study will be made available but may require execution of a materials transfer agreement. Source data are provided herein.

Acknowledgements We thank Stephen Goff and Brandon DeKosky for helpful discussions. This study was supported by funding from Andrew & Peggy Cherng, Samuel Yin, Barbara Picower and the JPB Foundation, Brie Biosciences, Roger & David Wu, and the Bill and Melinda Gates Foundation.

Author contributions The study was conceptualized by D.D.H. The experiments were principally carried out by P.W., M.N., Y.H., L.L., and S.I. with able assistance from M.W., J.Y. Structural interpretations were made by Y.G., Z.S., L.S., and P.D.K. B.Z., P.D.K., and C.A.K. provided mAbs. J.Y.C. and M.T.Y. provided plasma from convalescent patients. B.S.G. and J.R.M. provided sera from participants in the Moderna vaccine trial; J.Y.C. and M.S. provided sera from health care workers immunized with the Pfizer vaccine. Y.H. and Y.L. helped to supervise the study. The manuscript was written by D.D.H. with editing by P.W., P.D.K., L.S., Y.L., and reviewed, commented, and approved by all the authors.

Competing interests P.W., L.L., J.Y., M.N., Y.H., and D.D.H. are inventors on a provisional patent application on mAbs to SARS-CoV-2. D.D.H. is a member of the scientific advisory board of Brie Biosciences, which also has provided a grant to Columbia University to support this and other studies on SARS-CoV-2.

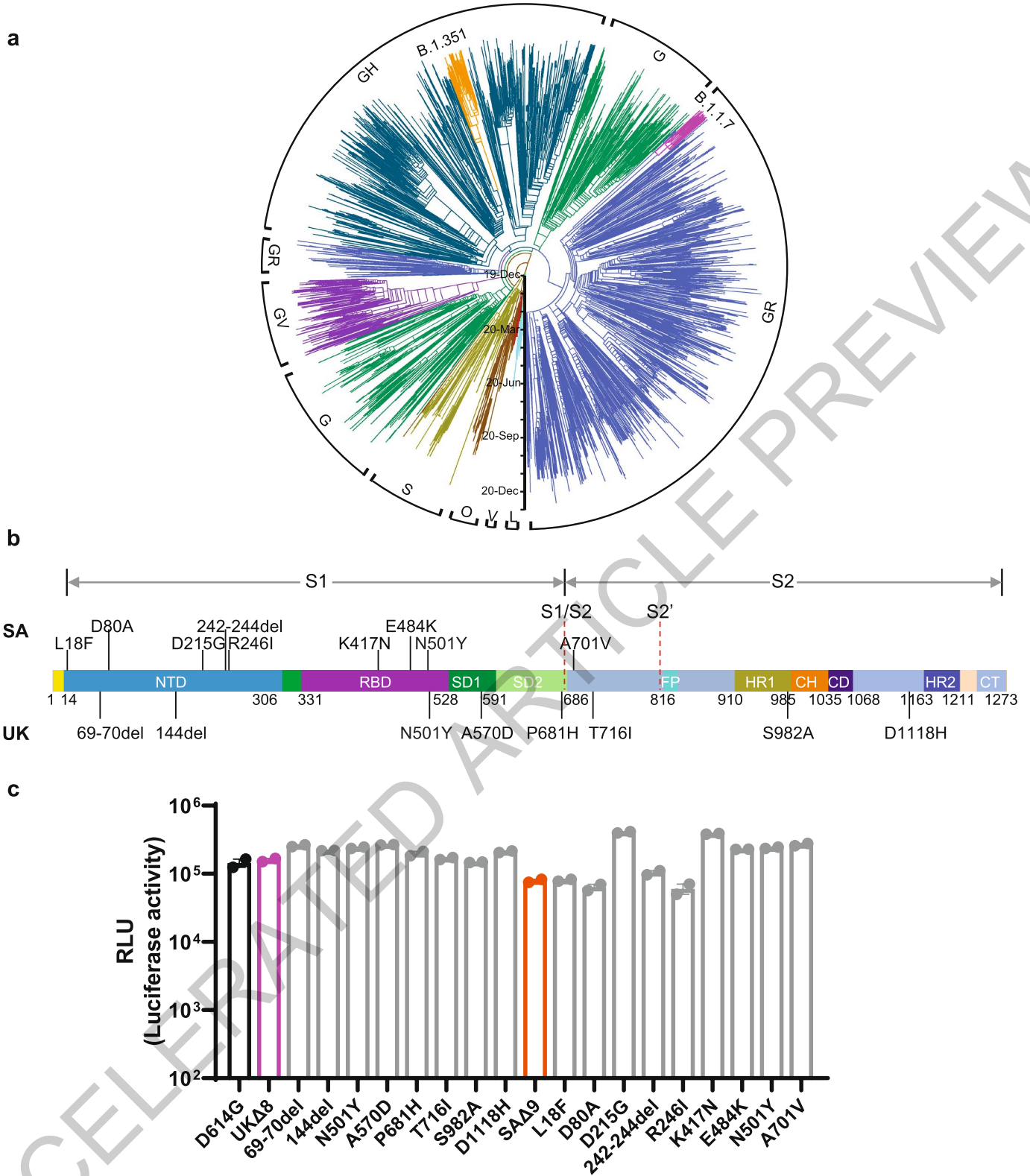
Additional information

Supplementary information The online version contains supplementary material available at <https://doi.org/10.1038/s41586-021-03398-2>.

Correspondence and requests for materials should be addressed to Y.H. or D.D.H.

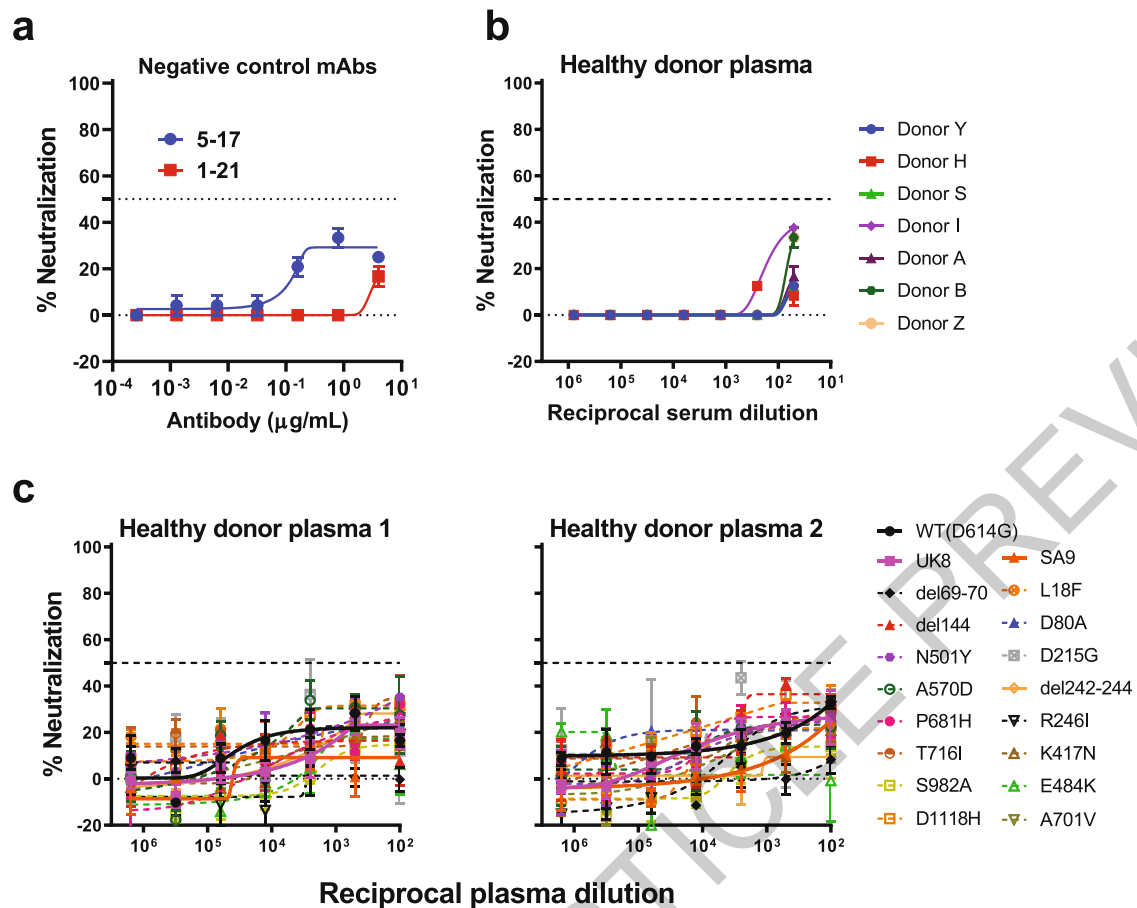
Peer review information Nature thanks Jesse Bloom, Andreas Radbruch and the other, anonymous, reviewer(s) for their contribution to the peer review of this work.

Reprints and permissions information is available at <http://www.nature.com/reprints>.



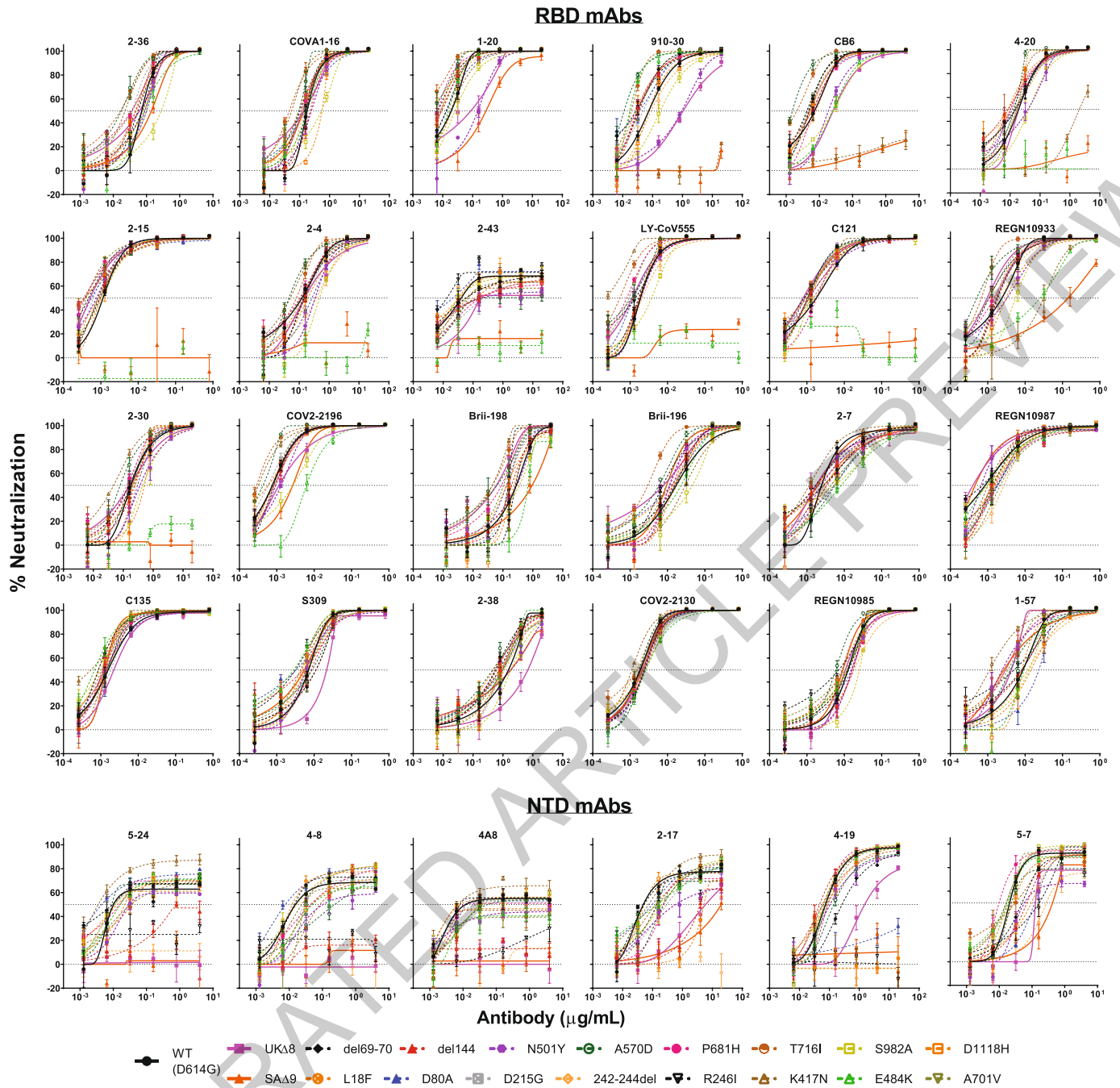
Extended Data Fig. 1 | Emerging SARS-CoV-2 variants identified in the United Kingdom and South Africa. **a**, Phylogenetic tree of SARS-CoV-2 variants, with B.1.351 and B.1.1.7 highlighted. **b**, Mutations in the viral spike identified in B.1.351 (SA) and B.1.1.7 (UK) in addition to D614G. **c**, Titers of WT (D614G) and the 18 mutant SARS-CoV-2 pseudoviruses. VSV-based

pseudoviruses were generated^{20,21} and viral particles were quantified and normalized by VSV nucleocapsid protein by western blot. Equal amount of each pseudovirus was then used to infect Vero E6 cells and relative luciferase unit (RLU) was measured 16 hrs later. Data represent mean \pm SEM of technical duplicates.

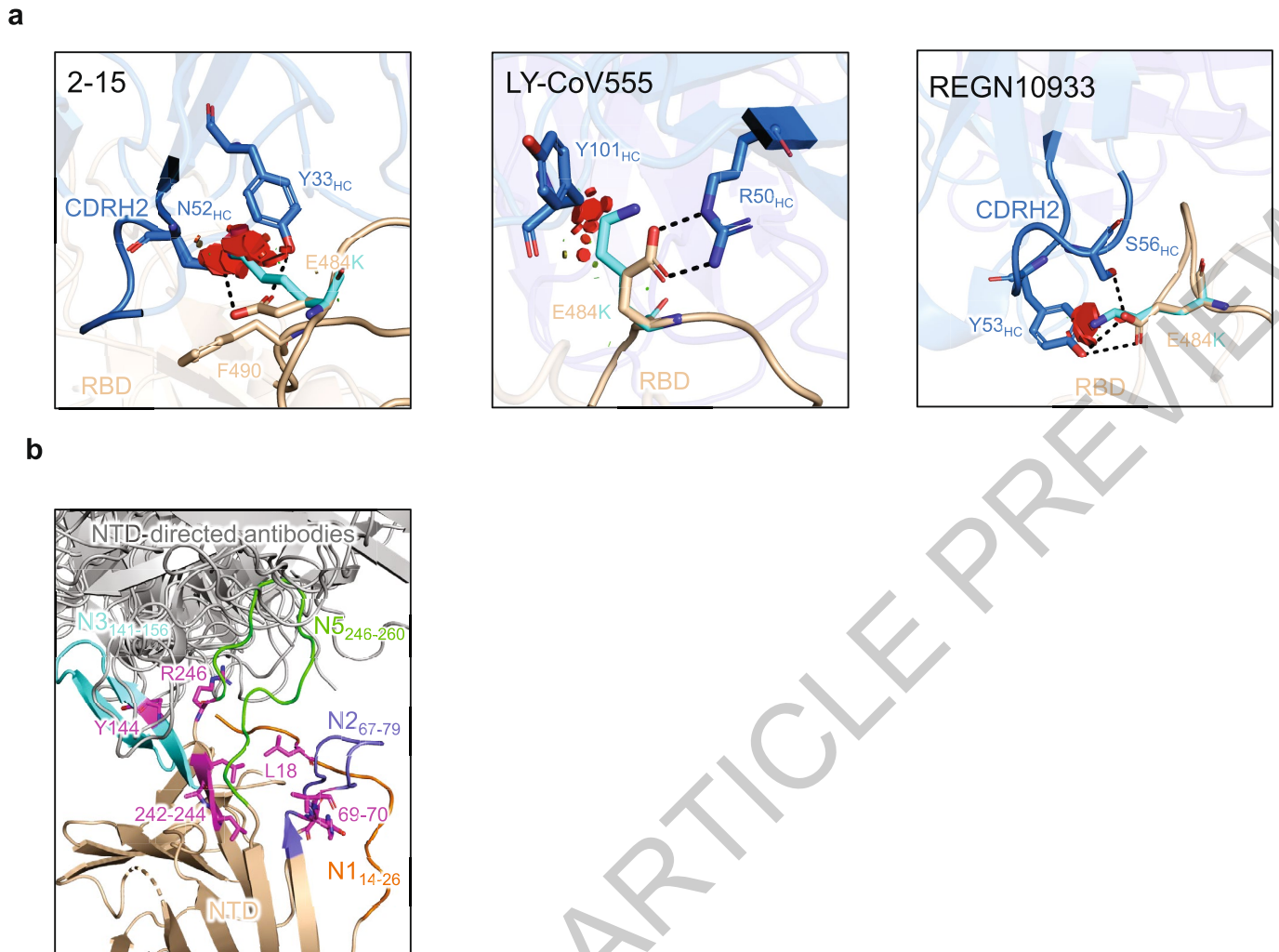


Extended Data Fig. 2 | Neutralization profiles of negative control mAbs and healthy donor plasma. **a**, Neutralization of two SARS-CoV-2 non-neutralizing mAbs²⁰ and **b**, healthy donor plasma against WT (WAI) live virus.

c, Neutralization of two healthy donor plasma against WT, UKΔ8, and SAΔ9, as well as single-mutation pseudoviruses. Data represent mean ± SEM of technical triplicates.

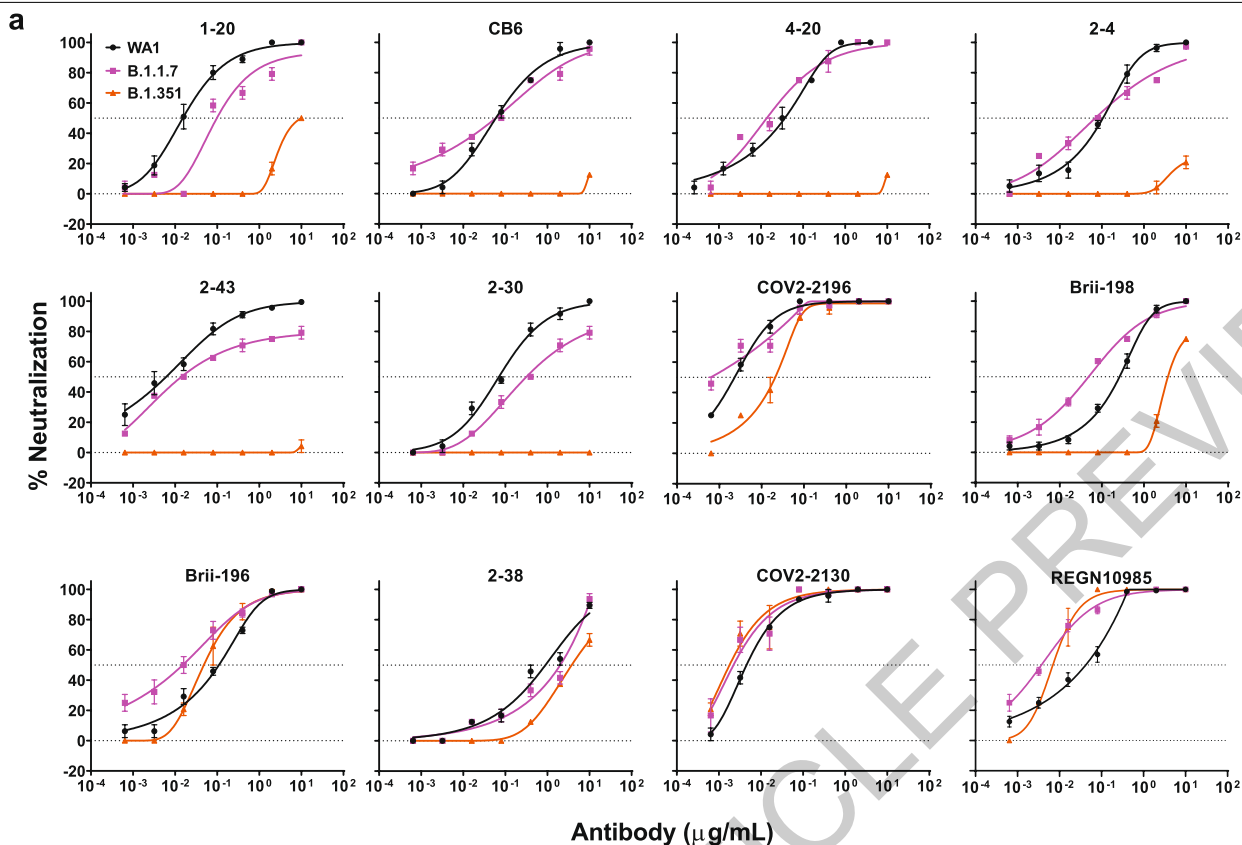


Extended Data Fig. 3 | Neutralization profiles of mAbs against WT, UKΔ8, and SAΔ9, as well as single-mutation pseudoviruses. Data represent mean \pm SEM of technical triplicates.



Extended Data Fig. 4 | Structural explanations on how critical mutations affect mAb activity. a, E484 forms hydrogen bonds with mAbs that target RBM. Mutation E484K causes not only steric clashes but also a charge change at antibody binding sites, and thus abolishes binding by these RBM-directed

mAbs. Steric clashes are shown by red plates. **b,** Mutations at or near the NTD antigenic supersite – comprised of loops N1, N3, and N5 – that is recognized by many potent NTD-directed mAbs.



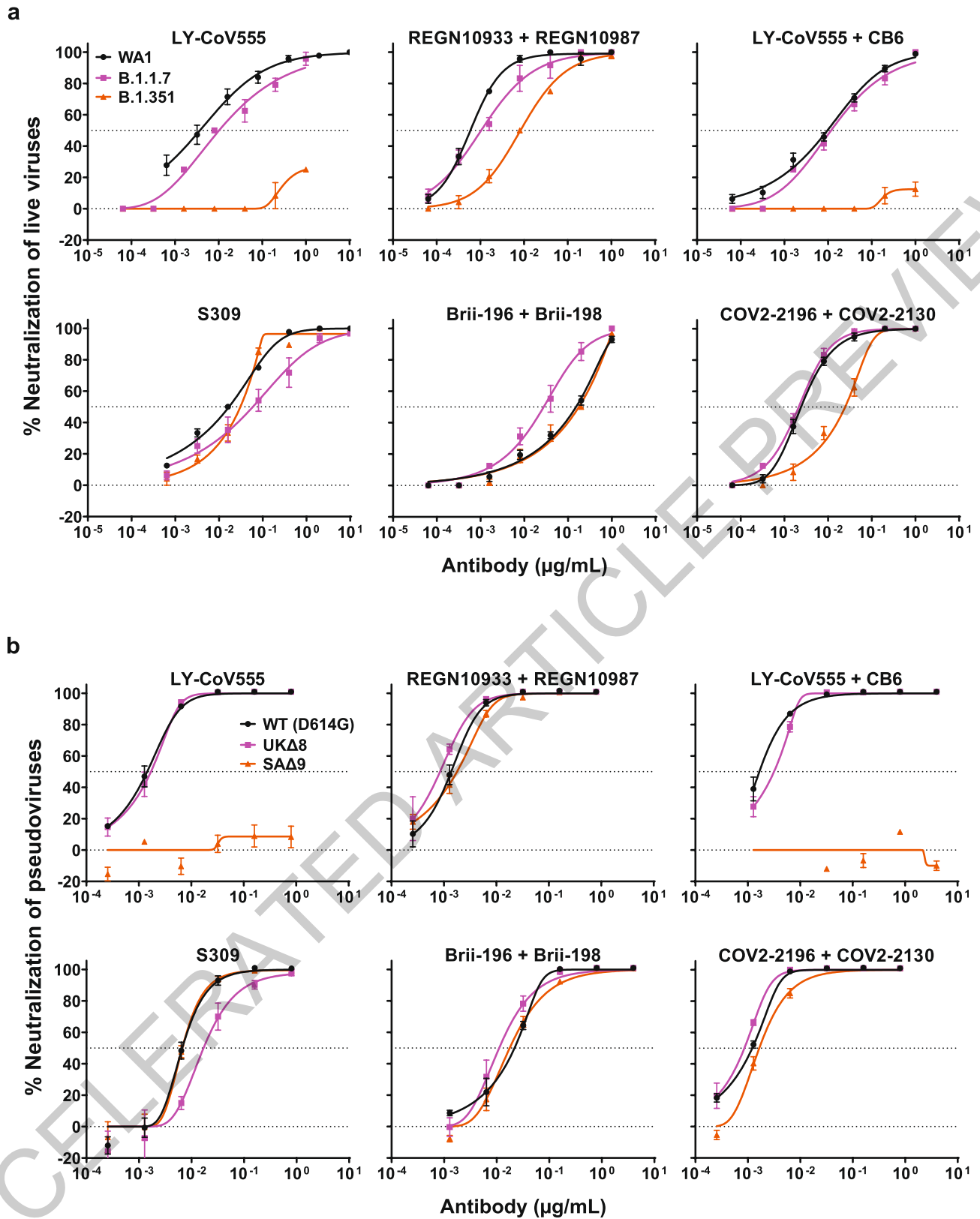
b

Fold change of IC50 from WT		RBD-directed mAbs											
		1-20	CB6	4-20	2-4	2-43	2-30	COV2-2196	Brij-198	Brij-196	2-38	COV2-2130	REGN10985
UK	B.1.1.7	-5.6	1.4	2.4	1.3	-2.3	-4.4	3.0	5.6	7.3	-1.8	3.0	10.5
	UKΔ8	-4.5	-3.6	-1.0	-1.2	-4.1	1.1	-1.5	4.6	2.2	-4.4	-1.1	1.2
	69-70del	1.5	1.5	1.2	-1.2	-1.4	1.1	1.0	1.1	1.1	2.8	-1.3	-1.0
	144del	2.2	1.2	2.2	-1.2	-3.7	-1.3	-1.1	1.4	1.2	1.6	-1.0	-1.4
	N501Y	-7.7	-2.6	-2.1	-2.8	-4.8	-2.0	-1.7	-1.0	1.5	-1.2	-1.3	-1.3
	A570D	4.6	4.6	1.4	2.7	-5.3	2.3	1.8	4.4	2.9	3.4	1.1	2.1
	P681H	2.9	1.1	1.8	1.2	-4.5	1.3	-1.2	3.1	1.5	2.7	-1.4	-1.3
	T716I	10.0	3.4	1.9	1.5	-1.5	-1.1	2.6	6.3	5.7	1.7	1.2	1.4
	S982A	-1.3	-3.6	-2.2	-3.9	1.2	-2.4	-3.6	-1.3	-2.7	-1.2	-1.4	-2.0
D1118H	1.0	1.4	1.1	-1.6	1.2	-2.8	1.3	1.2	1.2	1.8	-1.2	1.0	
SA	B.1.351	-667.0	<-1000	<-1000	<-1000	<-1000	<-1000	-6.3	-14.6	2.2	-3.5	3.0	5.3
	SAΔ9	-14.4	<-1000	<-1000	<-1000	<-1000	<-1000	-3.5	-3.4	1.8	-1.2	-1.0	1.4
	L18F	2.2	1.3	2.2	-1.0	-2.8	-1.1	1.0	2.1	1.1	3.1	-1.2	1.1
	D80A	1.4	1.4	1.6	-2.4	1.9	-1.1	-1.2	2.1	1.4	1.6	-1.0	-1.2
	D215G	2.4	1.6	1.3	-1.4	-5.6	1.4	1.3	1.7	1.0	1.5	1.1	1.4
	242-244del	5.1	-1.1	1.5	-2.1	1.2	1.1	1.0	1.7	-1.1	1.4	1.3	-1.4
	R246I	2.8	1.7	1.3	-1.1	3.0	1.2	-1.1	1.9	2.3	2.0	-1.2	1.8
	K417N	1.1	<-1000	-108.3	2.5	-1.7	3.8	2.4	6.3	-1.8	2.5	1.7	1.1
	E484K	1.3	-3.5	<-1000	<-1000	<-1000	<-1000	-8.1	-2.5	-1.4	1.5	-1.4	1.0
	N501Y	-7.7	-2.6	-2.1	-2.8	-4.8	-2.0	-1.7	-1.0	1.5	-1.2	-1.3	-1.3
A701V	2.1	1.6	1.1	1.1	-1.6	-1.2	-1.1	2.7	1.8	1.7	-1.0	1.2	

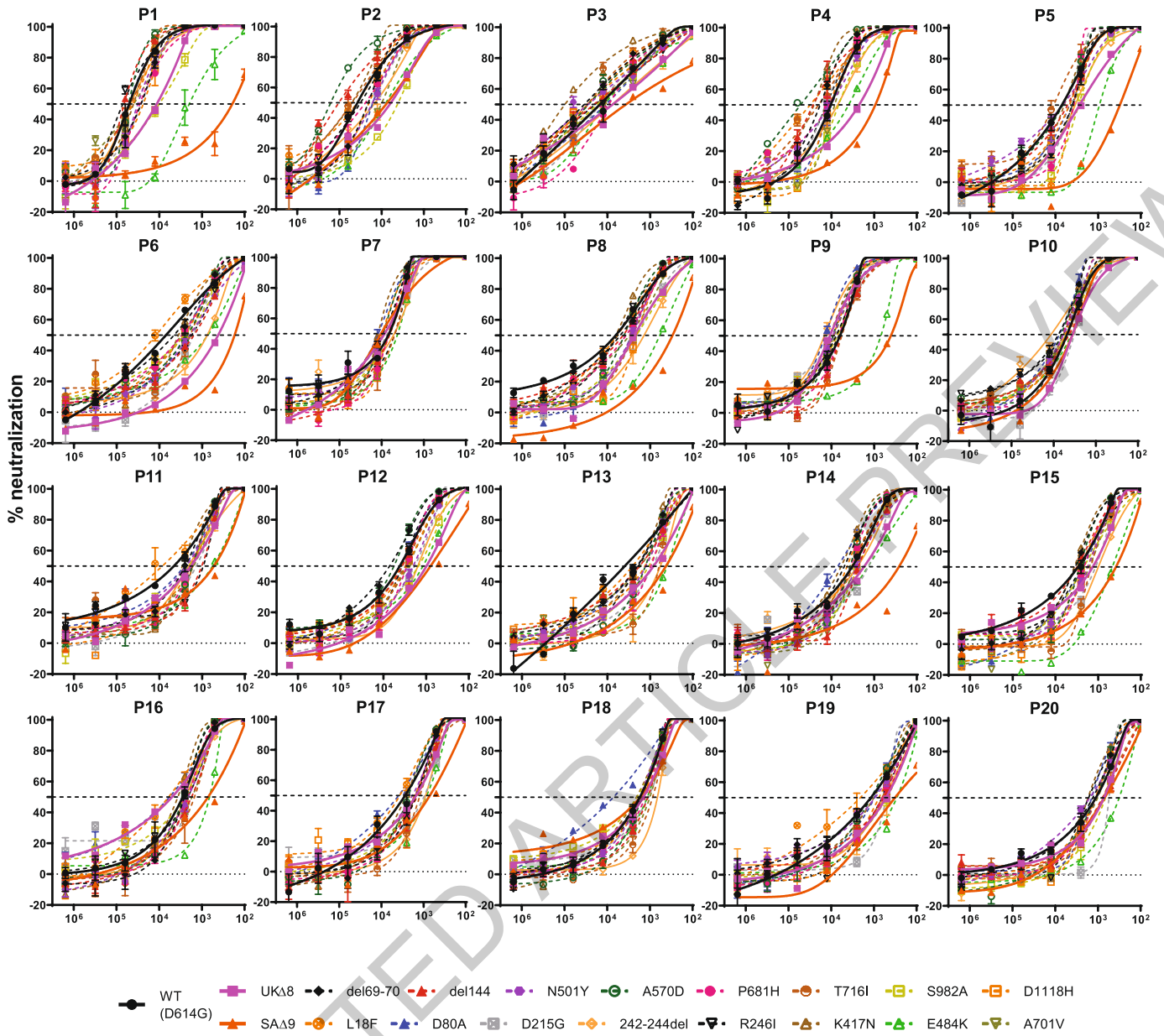
Red: resistance >3 fold; Green: sensitization >3 fold

Extended Data Fig. 5 | Neutralization susceptibility of UK and SA variants to additional SARS-CoV-2 RBD-directed mAbs. a, Neutralization of B.1.1.7, B.1.351, and WT viruses by additional RBD-directed mAbs. Data represent

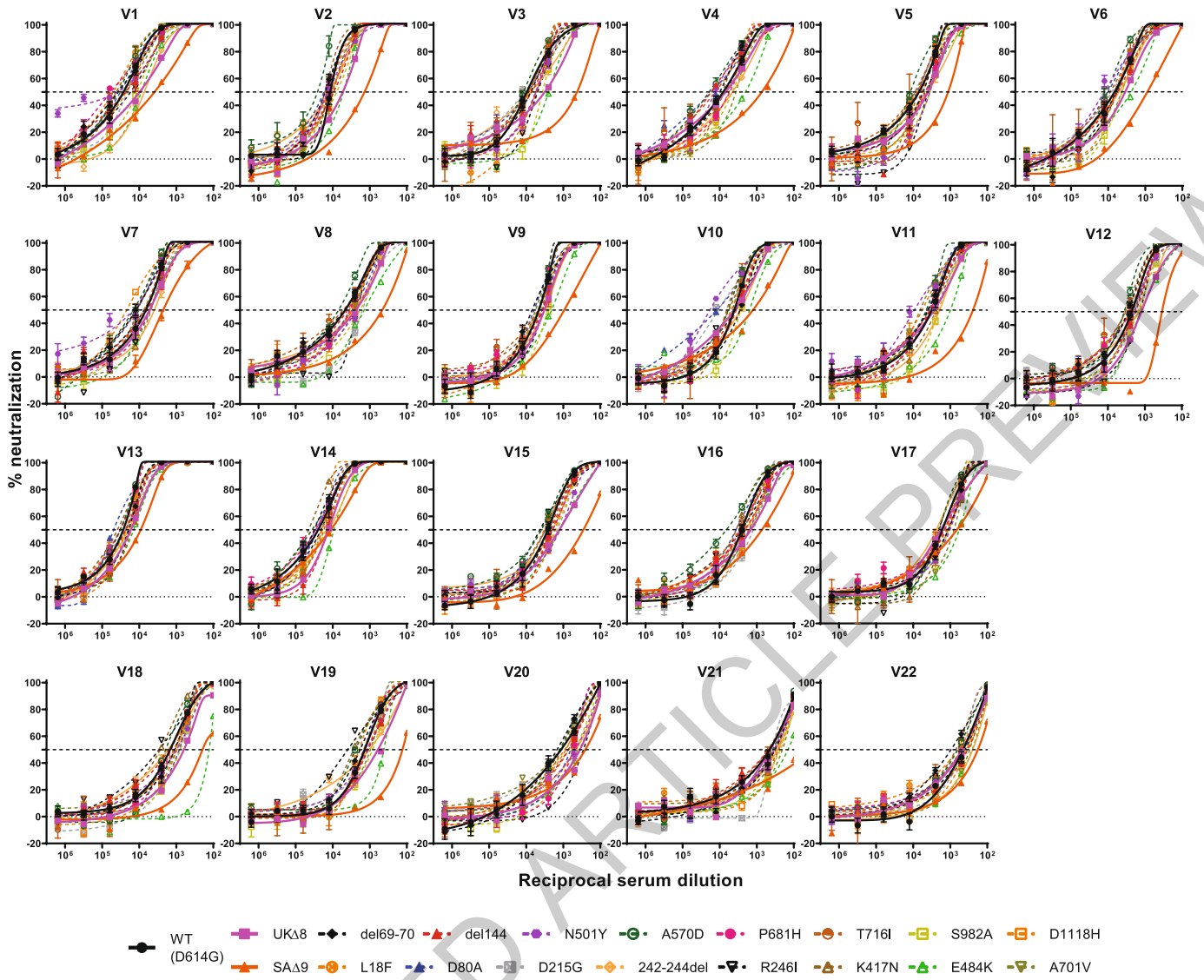
mean ± SEM of technical triplicates. b, Fold increase or decrease in IC50 of neutralizing mAbs against B.1.1.7 and B.1.351, as well as mutant pseudoviruses, relative to WT.



Extended Data Fig. 6 | Neutralization profiles of authorized or investigational therapeutic mAbs against WT (WA1), B.1.1.7, and B.1.351 live viruses (a), and against WT, UKΔ8, and SAAΔ9 pseudoviruses (b). Data represent mean \pm SEM of technical triplicates.



Extended Data Fig. 7 | Neutralization profiles of 20 convalescent patient plasma against WT, UKΔ8, SAΔ9, and single-mutation pseudoviruses. Data represent mean ± SEM of technical triplicates. Neutralization by health donor plasma is shown in Extended Data Fig. 2c.



Extended Data Fig. 8 | Neutralization profiles of vaccinee sera against WT, UKΔ8, SAΔ9, and single-mutation pseudoviruses. 12 sera from Moderna vaccinees (V1-V12) and 10 sera from Pfizer vaccinees (V13-V22) were tested. Data represent mean \pm SEM of technical triplicates.

Reporting Summary

Nature Research wishes to improve the reproducibility of the work that we publish. This form provides structure for consistency and transparency in reporting. For further information on Nature Research policies, see our [Editorial Policies](#) and the [Editorial Policy Checklist](#).

Statistics

For all statistical analyses, confirm that the following items are present in the figure legend, table legend, main text, or Methods section.

- | n/a | Confirmed |
|-------------------------------------|--|
| <input type="checkbox"/> | <input checked="" type="checkbox"/> The exact sample size (n) for each experimental group/condition, given as a discrete number and unit of measurement |
| <input type="checkbox"/> | <input checked="" type="checkbox"/> A statement on whether measurements were taken from distinct samples or whether the same sample was measured repeatedly |
| <input type="checkbox"/> | <input checked="" type="checkbox"/> The statistical test(s) used AND whether they are one- or two-sided
<i>Only common tests should be described solely by name; describe more complex techniques in the Methods section.</i> |
| <input checked="" type="checkbox"/> | <input type="checkbox"/> A description of all covariates tested |
| <input checked="" type="checkbox"/> | <input type="checkbox"/> A description of any assumptions or corrections, such as tests of normality and adjustment for multiple comparisons |
| <input type="checkbox"/> | <input checked="" type="checkbox"/> A full description of the statistical parameters including central tendency (e.g. means) or other basic estimates (e.g. regression coefficient) AND variation (e.g. standard deviation) or associated estimates of uncertainty (e.g. confidence intervals) |
| <input type="checkbox"/> | <input checked="" type="checkbox"/> For null hypothesis testing, the test statistic (e.g. F , t , r) with confidence intervals, effect sizes, degrees of freedom and P value noted
<i>Give P values as exact values whenever suitable.</i> |
| <input checked="" type="checkbox"/> | <input type="checkbox"/> For Bayesian analysis, information on the choice of priors and Markov chain Monte Carlo settings |
| <input checked="" type="checkbox"/> | <input type="checkbox"/> For hierarchical and complex designs, identification of the appropriate level for tests and full reporting of outcomes |
| <input checked="" type="checkbox"/> | <input type="checkbox"/> Estimates of effect sizes (e.g. Cohen's d , Pearson's r), indicating how they were calculated |

Our web collection on [statistics for biologists](#) contains articles on many of the points above.

Software and code

Policy information about [availability of computer code](#)

Data collection

Data analysis

For manuscripts utilizing custom algorithms or software that are central to the research but not yet described in published literature, software must be made available to editors and reviewers. We strongly encourage code deposition in a community repository (e.g. GitHub). See the Nature Research [guidelines for submitting code & software](#) for further information.

Data

Policy information about [availability of data](#)

All manuscripts must include a [data availability statement](#). This statement should provide the following information, where applicable:

- Accession codes, unique identifiers, or web links for publicly available datasets
- A list of figures that have associated raw data
- A description of any restrictions on data availability

Field-specific reporting

Please select the one below that is the best fit for your research. If you are not sure, read the appropriate sections before making your selection.

Life sciences Behavioural & social sciences Ecological, evolutionary & environmental sciences

For a reference copy of the document with all sections, see [nature.com/documents/nr-reporting-summary-flat.pdf](https://www.nature.com/documents/nr-reporting-summary-flat.pdf)

Life sciences study design

All studies must disclose on these points even when the disclosure is negative.

Sample size	We obtained convalescent plasma from 20 patients, vaccinee sera from 12 Moderna SARS-Co-2 mRNA-1273 Vaccine participants and 10 Pfizer BNT162b2 Covid-19 Vaccine participants. The sample size is appropriate within technical capability to compare the difference between groups
Data exclusions	No data were excluded from the analysis
Replication	Studies that were repeated are noted in figure captions and include all studies that demonstrated the key results reported in the manuscript.
Randomization	Randomization is not relevant as this is an observational study.
Blinding	The investigators were not blinded as this is an observational study.

Reporting for specific materials, systems and methods

We require information from authors about some types of materials, experimental systems and methods used in many studies. Here, indicate whether each material, system or method listed is relevant to your study. If you are not sure if a list item applies to your research, read the appropriate section before selecting a response.

Materials & experimental systems

n/a	Involved in the study
<input type="checkbox"/>	<input checked="" type="checkbox"/> Antibodies
<input type="checkbox"/>	<input checked="" type="checkbox"/> Eukaryotic cell lines
<input checked="" type="checkbox"/>	<input type="checkbox"/> Palaeontology and archaeology
<input checked="" type="checkbox"/>	<input type="checkbox"/> Animals and other organisms
<input type="checkbox"/>	<input checked="" type="checkbox"/> Human research participants
<input checked="" type="checkbox"/>	<input type="checkbox"/> Clinical data
<input checked="" type="checkbox"/>	<input type="checkbox"/> Dual use research of concern

Methods

n/a	Involved in the study
<input checked="" type="checkbox"/>	<input type="checkbox"/> ChIP-seq
<input checked="" type="checkbox"/>	<input type="checkbox"/> Flow cytometry
<input checked="" type="checkbox"/>	<input type="checkbox"/> MRI-based neuroimaging

Antibodies

Antibodies used	Monoclonal antibodies tested in this study were constructed and produced at Columbia University as previously described ²⁰ , except REGN10933, REGN10987, REGN10985, COV2-2196, and COV2-2130 were provided by Regeneron Pharmaceuticals, Inc., Brie-196 and Brie-198 were provided by Brie Biosciences, and CB6 was provided by B.Z. and P.D.K. Most mAbs were serially diluted (5-fold dilutions) starting at 10 µg/mL. Some clinical antibodies were tested from starting concentrations of 1 µg/mL.
Validation	All of the SARS-CoV2 spike antigen-specific monoclonal antibodies have been validated by binding to SARS-CoV-2 spike and neutralizing SARS-CoV-2 pseudovirus in previous publications cited in this paper.

Eukaryotic cell lines

Policy information about [cell lines](#)

Cell line source(s)	In this study we used the following cell lines: Vero E6 (ATCC, Cat# CRL-1586) and HEK293T (ATCC Cat# CRL-3216).
Authentication	All cell lines were obtained from authenticated vendors. Cells were recovered as healthy logarithmically growing cells within 4 to 7 days after thawing. Viability was measured and found to be >90%.
Mycoplasma contamination	Mycoplasma is negative (Detected mycoplasma contamination using Mycoplasma PCR ELISA ,Sigma,catalog number is 11663925910)
Commonly misidentified lines (See ICLAC register)	None

Human research participants

Policy information about [studies involving human research participants](#)

Population characteristics	Plasma samples were obtained from patients (age 34-79; mean 54) convalescing from documented SARS-CoV-2 infection approximately one month after recovery or later.
Recruitment	Convalescing patients volunteered for the cohort study. These cases were enrolled into an observational cohort study of convalescent patients followed at the Columbia University Irving Medical Center starting in the Spring of 2020. From their documented clinical profiles, plasma samples from ten with severe Covid-19 were selected, along with plasma from 10 with non-severe infection, for this study.
Ethics oversight	The study protocol was approved by the CUIMC Institutional Review Board (IRB), and all participants provided written informed consent. Sera were obtained from 12 participants in a Phase 1 clinical trial of Moderna SARS-CoV-2 mRNA-1273 Vaccine conducted at the NIH, under a NIH IRB-approved protocol. Sera were also obtained from 10 individuals followed in a CUIMC IRB-approved protocol to assess immunological responses to SARS-CoV-2 who received the Pfizer BNT162b2 Covid-19 Vaccine as a part of the emergency use authorization.

Note that full information on the approval of the study protocol must also be provided in the manuscript.